AN INVESTIGATION OF THE VALIDITY CRITERIA FOR LOCAL THERMODYNAMIC EQUILIBRIUM IN A NITROGEN PLASMA

by

J. P. S. RASH

A thesis submitted in partial fulfilment
of the requirements for the degree
of Master of Science in Physics
at the University of Cape Town

October, 1973

By nature the elements Earth, Water, Air and Fire exist; Fire and Air are forms of the body moving towards the limit; of all bodies, Fire is the finest.

- Aristotle, 437 B.C.

..... A world where matter may exist in a fourth state, where we can never enter and with which we must be content to observe and experiment from the outside.

- Sir William Crookes, 1879

CONTENTS

CHAPTER 1

INTRODUCTION: ATOMIC PROCESSES AND PLASMA MODELS

Local thermodynamic equilibrium (LTE) is said to hold in a plasma when collisional processes, balancing among themselves, dominate in atomic excitation and ionization equilibria. This requires the electron density to be high enough to provide sufficiently rapid collisional rates. (The electron density is the important parameter because of the dominant role of the electrons in collisional processes for plasmas with a degree of ionization greater than ~1%). It is the purpose of this thesis to examine the conditions under which LTE is valid, in a nitrogen plasma in particular.

1.1 Atomic Processes

In the LTE regime, because of the balancing of the (collisional) excitation and ionization processes with their inverses, the properties of the plasma are determined by the two parameters N_e (electron density) and T_e (electron temperature), as well as the chemical composition. Outside this regime, i.e. at lower densities, the various processes need to be considered in detail to determine the equilibrium state of the plasma, particularly if we wish to study the plasma by means of emitted line radiation, since this depends on level populations.

For an atomic species S^z, charge z, and ionization-recombination equilibrium $S^{z-1} \rightleftharpoons S^z + e$, the following processes need to be considered (p and q represent specific states in S^z or S^{z-1}):

(i) collisional ionization

$$S^{z-1}(q) + e \longrightarrow S^z(p) + e + e$$

and its inverse

(ii) three-body recombination

$$S^z(p) + e + e \longrightarrow S^{z-1}(q) + e$$

(iii) photo ionization

$$S^{z-1}(q) + h\nu \longrightarrow S^{z}(p) + e$$

and its inverse

(iv) radiative recombination

$$S^{z}(p) + e \longrightarrow S^{z-1}(q) + h\nu$$

(v) collisional excitation

$$S^{z-1}(q) + e \longrightarrow S^{z-1}(p) + e$$

and its inverse

(vi) collisional de-excitation

$$S^{z-1}(p) + e \longrightarrow S^{z-1}(q) + e$$

(vii) photo-excitation

$$S^{z-1}(q) + h\nu \longrightarrow S^{z-1}(p)$$

and its inverse

(viii) spontaneous and stimulated emission

$$S^{z-1}(p) \longrightarrow S^{z-1}(q) + h\nu$$

(ix) auto-ionization (from a doubly excited state n)

$$S^{z-1}_{**}(n) \longrightarrow S^{z}(p) + e$$

and its inverse

(x) dielectronic recombination

$$S^{z}(p) + e \longrightarrow S^{z-1}_{**}(n) \longrightarrow S^{z-1}(q) + h\nu$$

(q below the ionization limit)

Processes (ix) and (x) can obviously occur in non-hydrogenic systems only. For an optically thin plasma, as is assumed in our case, processes (iii) and (vii) and stimulated emission are neglected; thus complete thermodynamic equilibrium (where detailed balancing holds; i.e. each process is balanced by its inverse) is never attainable in such a plasma, as (iv) and (viii) are unbalanced.

1.2 Plasma Models

The rate of three-body (collisional) recombination (process (ii)) is proportional to N_e^2, while that for radiative recombination (process (iv)) is proportional to N_e. Thus (ii) is the dominant process for high N_e while (iv) dominates at low values. When the former is true, and in addition (vi) is the dominant de-excitation mechanism ((ix) and (x) are generally negligible compared with the other processes), we have an LTE model plasma, and "the population densities in the specific quantum states are those pertaining to a system in complete thermodynamic equilibrium which has the same total density, temperature and chemical composition as the actual system" (Griem (1962)). Under these conditions the population N_p^z of state p in ionization stage z of a species is given relative to the ground state population N_1^z by the Boltzmann equation

$$\frac{N_p^z}{N_1^z} = \frac{g_p^z}{g_1^z} \exp - \frac{E_p^z}{kT_e} \qquad (1.1)$$

where g_p^z, g_1^z are the respective statistical weights and E_p^z is the (positive) excitation energy of level p relative to the ground state. In addition, the ionization equilibrium is then determined by Saha's equation

$$\frac{N_1^z N_e}{N_1^{z-1}} = 2\left(\frac{m_e kT_e}{2\pi\hbar^2}\right)^{3/2} \frac{g_1^z}{g_1^{z-1}} \exp - \frac{E_\infty^{z-1}}{kT_e} \qquad (1.2)$$

where E_∞^{z-1} is the ionization energy of ionization stage z-1. (The relative total ion populations N_a^z, N_a^{z-1} are given by the same equation with g_1^z and g_1^{z-1} replaced by the partition functions $U^z(T_e) = \sum_p g_p^z \exp - \frac{E_p^z}{kT_e}$ (1.3) and $U^{z-1}(T_e)$ respectively).

A level p is said to be in "partial LTE" when it has an LTE population, and an ion is said to be in "complete LTE" when all levels in that ion have LTE populations.

At low densities when radiative recombination (process (iv)) dominates over (ii) and balances (i), while spontaneous emission ("radiative de-excitation")

dominates over (vi) and balances (v), the plasma is in Corona equilibrium (so called because this is the situation in the solar corona), a model originally proposed by Woolley and Allen (1948). The relative level populations are then given by

$$\frac{N_p^z}{N_1^z} = \frac{N_e K_{1p}^z}{A_p^z} \qquad (1.4)$$

where K_{1p}^z is the rate coefficient for collisional excitation from the ground state to p, and $A_p^z = \sum_{q<p} A_{pq}^z$, A_{pq}^z being the spontaneous transition probability for the transition $p \longrightarrow q$. (Collisional excitation from the ground state only is considered because A_p^z is large so that the populations of the excited states, $p > 1$, will be small; this "coronal approximation" should of course be checked under particular conditions). Similarly, the ionization equilibrium is given by

$$\frac{N_a^z}{N_a^{z-1}} = \frac{S^{z-1}}{\alpha^z} \qquad (1.5)$$

where S^{z-1} is the (total) collisional ionization coefficient from the ground state of z-1 to all levels of the continuum, and $\alpha^z = \sum_p \alpha_p^z$, α_p^z being the radiative recombination coefficient for the transition from the ground state of ionization stage z to level p of z-1. (The coronal approximation is again assumed). It is important to note that the RHS of (1.5) does not contain N_e, i.e. the ionization ratio is dependent only on temperature, in contrast to the Saha equation for the LTE situation which gives a dependence on N_e^{-1}.

For conditions between the domains of applicability of these two models the situation is more complex and all the atomic processes have to be considered in determining the ionization equilibrium and level populations. A generalised model, the collisional-radiative model, introduced by Bates, Kingston and McWhirter (1962), which tends to the LTE model at high densities and the Corona model at low densities, has been developed in an attempt to describe conditions in this region. This model is the subject of the next chapter.

CHAPTER 2

THE COLLISIONAL - RADIATIVE MODEL ; RATE COEFFICIENTS

2.1 The Collisional - Radiative Model for Hydrogenic Ions

Here we consider the ionization equilibrium $S^{z-1} \rightleftharpoons S^z + e$ with S^z a bare nucleus, charge z. Let p,q denote levels in the hydrogenic ion S^{z-1}, and c the continuum. Then we define the following process rates R and rate coefficients K, etc:

$$R^C_{pc} = N_p N_e K_{pc} \qquad \text{(collisional ionization } p \rightarrow c\text{)}$$

$$R^C_{pq} = N_p N_e \sum_{q \neq p} K_{pq} \qquad \text{(collisional excitation } (q>p) \text{ and de-excitation } (q<p),\ p \rightarrow \text{all other q)}$$

$$R^R_{pq} = N_p \sum_{q<p} A_{pq} \qquad \text{(spontaneous decay } p \rightarrow \text{ all } q<p\text{)}$$

$$R^C_{qp} = N_e \sum_{q \neq p} N_q K_{qp} \qquad \text{(collisional excitation } (q<p) \text{ and de-excitation } (q>p),\ \text{all other } q \rightarrow p\text{)}$$

$$R^R_{qp} = \sum_{q>p} N_q A_{qp} \qquad \text{(spontaneous decay all } q>p \rightarrow p\text{)}$$

$$R^C_{cp} = N^z N_e K_{cp} \qquad \text{(collisional recombination } c \rightarrow p\text{)}$$

$$R^R_{cp} = N^z N_e \beta_p \qquad \text{(radiative recombination } c \rightarrow p\text{)}$$

(N^z and N_e are the ion (bare nucleus) and electron densities respectively).

Then the rate of population of level p is given by

$$\dot{N}_p = -R^C_{pc} - R^C_{pq} - R^R_{pq} + R^C_{qp} + R^R_{qp} + R^C_{cp} + R^R_{cp} \qquad (2.1)$$

Radiative excitation and ionization are omitted because the plasma is optically thin by assumption; auto-ionization and di-electronic recombination do not occur in hydrogenic systems.

We now basically follow the formulation of Bates, Kingston and McWhirter (1962) (hereafter referred to as BKM).

Substitution for the R's in equations of the form (2.1) for all levels p yields an infinite system of coupled differential equations (DE's) which determine the course of recombination with respect to time.

For the sake of convenience, each equation is normalised with respect to N_p^E, the LTE population of p (given by the Boltzmann and Saha equations). Then detailed balancing of the collisional processes in LTE allows the substitution of

$$\frac{N_p^E}{N_q^E} K_{pq} \quad \text{for} \quad K_{qp}$$

and

$$\frac{N_p^E}{N_q^E} K_{pc} \quad \text{for} \quad K_{cp}.$$

Then defining

$$b_p = \frac{N_p}{N_p^E} \tag{2.2}$$

$$K_p = K_{pc} + \sum_{q \neq p} K_{pq} \tag{2.3}$$

$$A_p = \sum_{q<p} A_{pq} \tag{2.4}$$

and

$$X = \frac{N_e}{N^z} \tag{2.5}$$

the DE for level p becomes

$$\frac{\dot{N}_p}{N_p^E} = -b_p (N_e K_p + A_p) + \sum_{q \neq p} b_q N_e K_{pq} + \sum_{q>p} b_q \frac{N_q}{N_p^E} A_{pq} + N_e K_{pc} + \frac{N_e^2}{X N_p^E} \beta_p . \tag{2.6}$$

A number of simplifying assumptions are now introduced:

(i) Evaluation of the expression for N_p^E in numerical form (BKM eq. (12)) shows that under a wide range of plasma conditions,

$$N_p^E \ll N^z \text{ and } N_e, \; p>1 \tag{2.7}$$

(ii) It follows from (i) that under an even larger range of conditions

$$N_p \ll N_e, \; p>1 \tag{2.8}$$

At temperatures of the order of a few eV ($\sim 50\,000^{\circ}$K) this condition is only violated for extremely dense plasmas with

$$\frac{N_e}{Xz^3} = \frac{N^z}{z^3} \gtrsim 10^{19} \text{ cm}^{-3}.$$

(Incidentally, this condition also ensures that collisions may be regarded as distinct events).

(iii) If the mean thermal energy kT_e is very much less than the first excitation energy E_2^{z-1}, then

$$N_p \ll N_1, \; p>1 \tag{2.9}$$

in the steady state. Then a quasi-equilibrium is almost immediately established amongst the excited levels, which does not appreciably affect the number densities of free electrons and ions N_e and N^z. Once this quasi-equilibrium is established, "the rates at which excited systems are produced and destroyed by collisional and radiative processes are much greater than the rates at which the number densities of these rare systems change as the plasma decays" (BKM p. 300). Thus one essentially considers the balance between the ground state population N_1 and N_e and N^z in the approach to equilibrium.

This assumption means that the left hand sides (LHS) of the differential equations (2.6) for $p>1$ can effectively be put equal to zero ($\dot{N}_p$ is negligible compared

to the individual terms on the RHS).

(iv) Since the rate coefficients for the collisional processes increase with increasing p while those for the radiative processes decrease, at high enough p (p>s, say), collisional processes dominate and $N_p \approx N_p^E$, its Saha equilibrium population (i.e. $b_p \approx 1$, p>s). An infinite matrix is thus avoided.

This results in a system of s-1 equations in the relative level populations b_p, $1 < p \leq s$, the solutions of which may be written in the form

$$b_p = r_o(p) + r_1(p) b_1, \qquad (2.10)$$

taking b_1 as known, where the coefficients $r_o(p)$ and $r_1(p)$ are (positive definite) functions of N_e and T_e. These coefficients may be written in terms of the various rate coefficients [Fujimoto (1973) eqs. (12), (13), where

$$Z(p) = \frac{N_p^E}{N_e N^z}$$

in our notation; $C(p,q) \equiv K_{pq}$ (collisional excitation, q>p); $F(q,p) \equiv K_{qp}$ (collisional de-excitation, q<p); $\alpha(p) \equiv K_{cp}$ (collisional (three-body) recombination c→p) and $S(p) \equiv K_{pc}$ (collisional ionization p → c)].

2.2 CR Ionization and Recombination Coefficients

The differential equation for p = 1, which describes the ionization and recombination of the plasma, may be written in the form

$$\dot{N}_1 = -N_1 N_e S_{CR} + N^z N_e \alpha_{CR} \qquad (2.11)$$

where S_{CR} and α_{CR} are defined as the collisional-radiative (CR) ionization and recombination coefficients respectively. These coefficients may be written in terms of the individual rate coefficients as (Fujimoto (1973)):

$$S_{CR} = K_{1c} + \sum_{q=2}^{s} K_{1q} - \frac{1}{N_1^E} \sum_{q=2}^{s} N_q^E \, r_1(q) \left(K_{q1} - \frac{A_{q1}}{N_e} \right) \qquad (2.12)$$

and

$$\alpha_{CR} = N_e K_{c1} + \beta_1 + \frac{1}{N^z} \sum_{q=2}^{s} N_q^E \, r_o(q) \left(K_{q1} + \frac{A_{q1}}{N_e} \right) \qquad (2.13)$$

At equilibrium we have

$$\dot{N}_1 = - \dot{N}^z = 0$$

and from (2.11)

$$\frac{N^z}{N_1^{z-1}} = \frac{S_{CR}}{\alpha_{CR}} \qquad (2.14)$$

which may be compared with the Corona relation (equation (1.5); $N_a^{z-1} \approx N_1^{z-1}$ from (2.9)), where S and α are the <u>collisional</u> ionization and <u>radiative</u> recombination coefficients. Thus in the low density limit we should have $S_{CR} \longrightarrow S_1 = K_{1c}$ and $\alpha_{CR} \longrightarrow \alpha \equiv \beta = \sum_{p=1}^{s} \beta_p$, which can in fact be shown from (2.12) and (2.13).

Fujimoto (1973) shows that in the low density limit ($N_e \longrightarrow 0$), S_{CR} and α_{CR} tend to the constant values S and α and in addition the coefficient $r_o(p)$ tends to a constant value $r_o^o(p)$ for each p, while $r_1(p)$ tends to a value $r_1^o(p)$ which is proportional to N_e. He derives, using both exact and approximate expressions, limiting values of N_e below which $r_o(p)$ is within 10% of $r_o^o(p)$ and $r_1(p)$ is within 10% of $r_1^o(p)$, for p = 2 through 20. These values of N_e are then used to give similar limits for S_{CR} and α_{CR} to be within 10% of S and α respectively, which turn out to be equivalent to the Coronal limits given by McWhirter (1965).

In the high density limit ($N_e \longrightarrow \infty$), Fujimoto (1973) similarly obtains the limiting values of the coefficients, viz. $r_o^\infty(p)$ and $r_1^\infty(p)$. Then S_{CR} in the high density limit becomes

$$S_{CR}^\infty = K_{1c} + \sum_{q \geq 2} K_{1q} \, r_o^\infty(q) \qquad (2.15)$$

(a constant value), and α_{CR}^∞ (proportional to N_e) is obtained from

$$\frac{S_{CR}^{\infty}}{\alpha_{CR}^{\infty}} = \frac{N^z}{N_1^E} \qquad (2.16)$$

the Saha ionization ratio. The limiting density $N_e^{S\infty}$ above which S_{CR} is within 10% of S_{CR}^{∞} is shown to be

$$N_e^{S\infty} \approx \frac{A_{21}}{K_{21}} \qquad (2.17)$$

and the limiting value for α_{CR} is equal to $N_e^{S\infty}$. When $N_e > N_e^{S\infty}$ it is then shown that $b_p \approx 1$, all p, i.e. the atom is in complete LTE (all levels have Saha equilibrium populations). Thus $N_e^{S\infty}$ is the lower limit for complete LTE; in fact this turns out to be the same condition as that given by Griem (1964) which is considered in section 3.2.

The coefficients S_{CR} and α_{CR} and their ratio (i.e. the ionization ratio) are plotted against N_e for a number of different temperatures in Fig. 2-1 (a), (b) and (c) respectively, and the limiting N_e's for the Coronal and LTE approximations from Fujimoto's estimates are also shown. These are for hydrogen; for a hydrogenic ion charge z we have the following "scaling laws":

$$N_e \equiv \frac{N_e}{z^7}, \quad T_e \equiv \frac{T_e}{z^2}$$
$$S_{CR} \equiv S_{CR}\, z^3, \quad \alpha_{CR} \equiv \frac{\alpha_{CR}}{z} \qquad (2.18)$$

Hereafter we drop the subscript "CR" and in accordance with (2.14) take S/α to be synonymous with the ionization ratio under all conditions.

2.3 Non-Hydrogenic Ions

Although, as is apparent from the last section, S/α, etc. are fairly well established for hydrogenic ions, this is certainly not the case for non-hydrogenic ones, as the rate coefficients are very poorly known. In addition, auto-ionization and di-electronic recombination can now occur and need to be

Fig. 2-1 : C.R. RATE COEFFS.

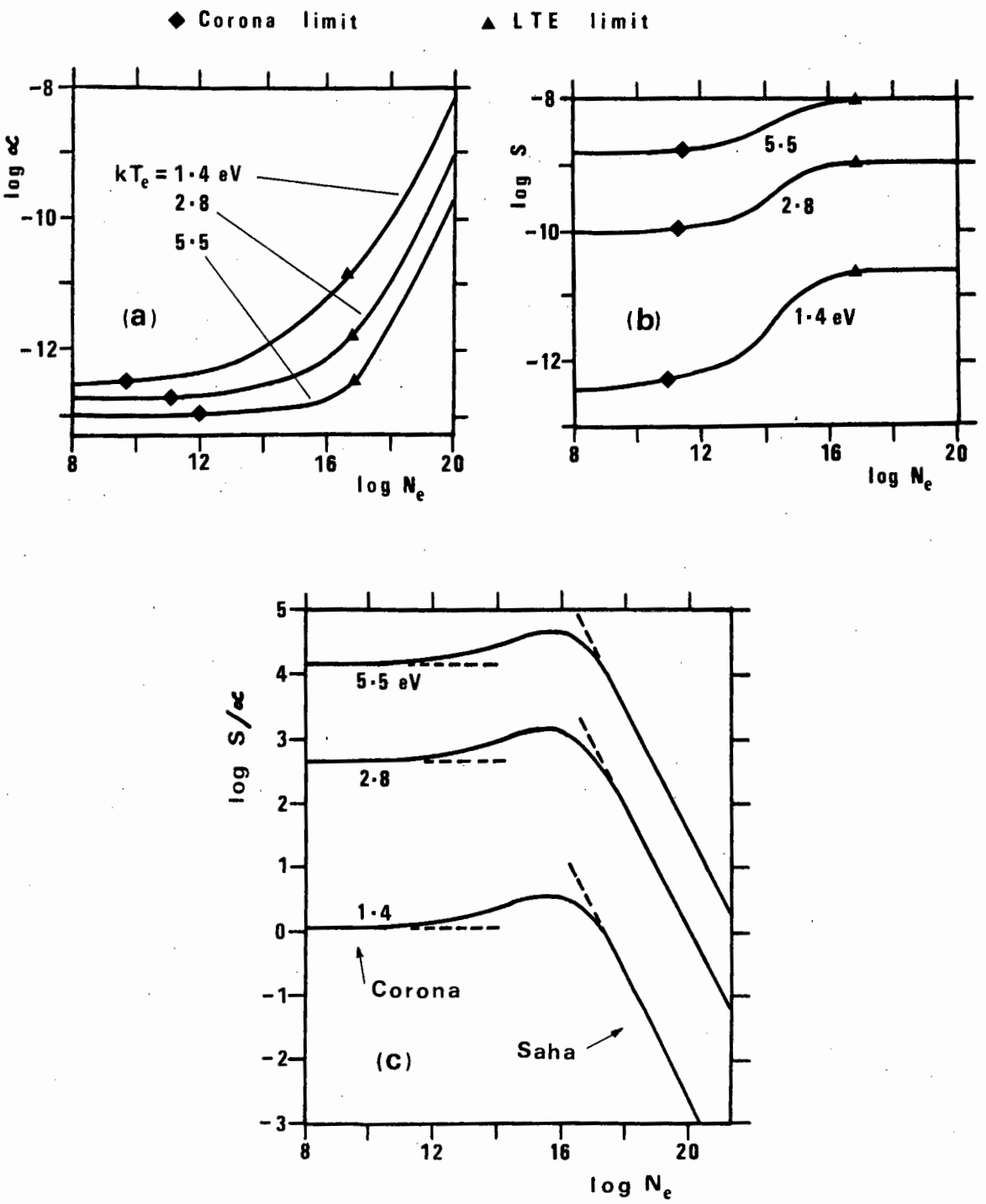

considered in determining the ionization equilibrium. Most of the work in this field is published in the astrophysics literature and considers the dependence of ionization equilibrium on temperature at low (Coronal) densities; the dependence of S/α on N_e at different temperatures is very poorly known.

House (1964) calculated the ionization equilibrium as a function of temperature for the elements H through Fe, including the processes of collisional ionization and collisional and radiative recombination. Tucker and Gould (1966) performed similar calculations, including also an approximate expression for di-electronic recombination. Jordan (1969) gives two sets of results for the elements C through Ni :

(i) including collisional ionization from the ground state, collisional excitation followed by auto-ionization, radiative recombination (direct and via bound levels), and di-electronic recombination "reduced by a density dependent term"; these results apply to the Solar Corona with an assumed model such that $N_e T_e \sim 10^{15}$ cm^{-3} ^{o}K;

(ii) including the same processes except that radiative recombination via bound levels is omitted and the full di-electronic recombination rate is used; these results apply to "any low density plasma where the radiation field is negligible".

Kulander (1965) uses a model of 26 levels through all eight ionization stages of nitrogen and determines the populations of these levels at $T_e = 10^4$, 10^5 and 10^6 ^{o}K and $N_e = 10^{11} - 10^{19}$ cm^{-3} in steps of 10^2 cm^{-3}. To observe the disparity in the different estimates, consider NIV/NIII at $T_e = 10^5$ ^{o}K ($kT_e = 8.6$ eV). Jordan's first (Coronal) set gives 4.6; the second ("low density") set gives 0.67, while Kulander gives values of about 80 for $N_e = 10^{11}$, 10^{13} and 10^{15} cm^{-3} for the total NIV/NIII. (According to Kulander the level "42", i.e. the 2s2p $^3P^o$ level at 8.4 eV in NIV has more than double the population of the ground state at this temperature; the ratio of ground state populations is about 40).

Park (1968) considers an optically thick nitrogen plasma at $N_e \sim 10^{15}$ cm $^{-3}$ and $5000 \leqslant T_e \leqslant 20\,000\ ^{o}K$ (i.e. $0.43 \leqslant kT_e \leqslant 1.9$ eV) where NI and NII are the dominant species assuming 41 "energy level groups" for NI.

The importance of auto-ionization and di-electronic recombination was pointed out by Burgess (1964, 1965); when these processes are included, the ratio of CR coefficients becomes

$$\frac{S_{tot}}{\alpha_{tot}} = \frac{S_{CR} + S_{auto}}{\alpha_{CR} + \alpha_{d}}$$

where S_{auto} and α_d are the respective rate coefficients. Cox and Tucker (1969) show that di-electronic recombination is most important for $10^5 \leqslant T_e \leqslant 10^6\ ^{o}K$ in a "low density" plasma, in considering the ionization equilibrium of the nine most naturally abundant elements (including nitrogen), and may affect the result by an order of magnitude in this region. However these processes are not expected to be important at the lower temperature of our regime.

CHAPTER 3

THEORETICAL LTE CRITERIA

Theoretical lower limits on N_e and kT_e for the applicability of partial (for a particular level) and complete LTE have been proposed by a number of authors. Wilson (1962) proposed a criterion in terms of the CR (collisional-radiative) model, using the thermal limit concept. Similar criteria were derived by Griem (1963) and McWhirter (1965); Drawin (1969) presented a modified version of Griem's criteria, and a derivation and review of these criteria in terms of the CR model has recently been given by Fujimoto (1973).

These criteria are generally formally derived for hydrogenic ions; Drawin (1969) considers generalisations to non-hydrogenic systems, while Kulander (1965) has presented estimates for nitrogen in particular. In this chapter we examine these criteria for partial and complete LTE in hydrogenic ions, their applicability to non-hydrogenic systems and nitrogen in particular, and consider the effects of possible reabsorption of resonance lines. Finally we examine the supplementary criteria for fulfilment of LTE.

3.1 Partial LTE of hydrogenic level p

We consider first the criteria for partial LTE of a level with principal quantum number p in a hydrogenic ion with nuclear charge Z. Following the formulation of Griem (1963), we say that level p is in partial LTE when the rate of collisional excitation (or ionization) to higher levels (or the continuum) is greater than that for radiative decay (or recombination) to lower levels, i.e.

$$N_e \sum_{q>p} C(p,q) > \sum_{q<p} A(p,q) \qquad (3.1)$$

Substitution of a classical cross-section, as given by Seaton (1962) (a reasonable approximation for ions) into C(p,q) yields as a condition for partial LTE of level p:

$$N_e \geq \frac{7.4 \times 10^{17} Z^7}{p^{17/2}} \sqrt{\frac{kT_e}{E_\infty^z}} \ \text{cm}^{-3} \qquad (3.2)$$

where E_∞^z ($=Z^2 E_H$) is the ionization potential of the (hydrogenic) ion.

Drawin (1969), using a semi-empirical cross-section, obtains the same result except for multiplication by a "quantum-mechanical correction"

$$\Psi^{-1}\left(\frac{2E^z}{p^3 kT_e}\right) .$$

The values of the monotonically decreasing function $\Psi(x)$ are tabulated, and result in N_e conditions a factor $\sim$4 higher than Griem's (1963) for low p, as well as a slightly different temperature dependence, and a factor $\sim$10 lower for levels $p \gtrsim 8$.

As an example, consider the level p = 4 in HeII (Z=2). (The upper level of the HeII line 4686 Å is $4f^2F^o$). At an electron temperature kT_e = 3 eV, equation (3.2) gives

$$N_e \geqslant 1.7 \times 10^{14} \text{ cm}^{-3}.$$

The variable $x = \dfrac{2E_\infty^z}{p^3 kT_e}$ in Drawin's correction factor $\Psi^{-1}(x)$ is 0.57 and Ψ (0.57) = 0.5, so that according to Drawin's formulation the above minimum density requirement should be increased by a factor 2.

An alternative formulation for partial LTE of a level p may be made in terms of the thermal limit concept. Wilson (1962) defined the thermal limit n_t (non-integral) as that level in the ion for which upward (predominantly collisional) and downward (predominantly radiative) transitions are equally probable; i.e. n_t is effectively the level at which equality holds in the inequality (3.1). Approximately the same values for n_t are obtained by defining it as the level at which the minimum total de-excitation rate (collisional + radiative) occurs, as was done by Byron et al. (1962).

Because of the decrease of the radiative rate and increase of the collisional rate with increasing quantum number, all levels above n_t will be in (partial) LTE.

For hydrogenic ions of nuclear charge Z, Wilson gives the following approximate expression for n_t:

$$n_t^7 = 1.5 \times 10^{17} \frac{Z^6}{N_e} \sqrt{kT_e} \qquad (3.3)$$

A more exact expression, from which n_t may be obtained by iteration, is given by Griem (1964):

$$n_t = 126 \frac{Z^{14/17}}{N_e^{2/17}} \left(\frac{kT_e}{Z^2 E_H} \right)^{1/17} \exp\left(\frac{4}{17} \frac{Z^2 E_H}{n_t^3 kT_e} \right) \qquad (3.4)$$

For example, in HeII (Z=2) at $kT_e = 3$ eV, $N_e = 10^{17}$ cm^{-3}, equation (3.3) gives $n_t = 2.08$, while (3.4) gives $n_t = 2.48$.

3.2 Complete LTE in a hydrogenic ion

Conditions for complete LTE in an ion can of course be obtained directly from those for partial LTE by extending the latter down to the ground state, i.e. putting p=1 in equation (3.2) or making the thermal limit n_t=1 so that collisional processes dominate for all levels in the ion. However, at or near complete LTE, the collisional population rate of the ground state becomes practically equal to its collisional depopulation rate (by detailed balancing), and the latter may be approximately equated to the partial rate to the upper state of the first resonance line.

Using the same classical cross-section as before, and equating the radiative population rate of the ground state to the radiative decay rate of the upper level of the resonance line, Griem (1963) derives as a condition for LTE down to the ground state

$$\left(\text{i.e. for } -\left.\frac{dN_1}{dt}\right|_{1 \to 2}^{\text{coll}} \geq -\left.\frac{dN_1}{dt}\right|_{1 \to 2}^{\text{rad}} \right),$$

$$N_e \geqslant 9.2 \times 10^{16} Z^7 \sqrt{\frac{kT_e}{E_\infty^Z}} \left(\frac{E_2 - E_1}{E_\infty^Z} \right)^3 \text{ cm}^{-3} \qquad (3.5)$$

$$= 1.05 \times 10^{16} Z^6 \sqrt{kT_e} \text{ cm}^{-3}$$

for a hydrogenic ion with nuclear charge Z, ionization potential $E_\infty^Z = Z^2 E_H$.

For example, for HeII (Z=2) at $kT_e = 3$ eV, equation (3.5) gives $N_e \geqslant 1.2 \times 10^{18}$ cm^{-3}.

Wilson (1962) derived a relation in terms of the ionization potential by extending the thermal limit down to the ground state; in the case of hydrogenic ions it reduces to the same as (3.5) apart from a slightly different numerical factor of 1.3×10^{17}.

3.3 Non-hydrogenic ions

For a general level system, Drawin (1969) considered the balance between a level p and the adjacent lower level q = p - 1 to determine whether p was in partial LTE. The two conditions to be fulfilled are: (i) the collisional de-excitation rate p → p - 1 is greater than the total spontaneous decay rate p → all lower levels; (ii) the collisional excitation rate p - 1 → p is greater than the total spontaneous decay rate p - 1 → all lower levels. Then collisional excitation compensates the enhanced decay rate of level p and the latter will be in partial LTE. This yields two conditions on N_e:

$$\text{(i)} \quad N_e \geqslant 1.15 \times 10^8 Z^3 \frac{g_p}{g_q} \frac{E_p - E_q}{E_\infty} \sqrt{\frac{kT_e}{E_\infty}} \frac{\sum_{m<p} A_{pm}}{f_{qp}} \bar{\Phi}\left(\frac{E_p - E_q}{kT_e}\right) \quad (3.6)$$

and

$$\text{(ii)} \quad N_e \geqslant 1.15 \times 10^8 Z^3 \frac{E_p - E_q}{E_\infty} \sqrt{\frac{kT_e}{E_\infty}} \frac{\sum_{m<q} A_{qm}}{f_{qp}} \Psi^{-1}\left(\frac{E_p - E_q}{kT_e}\right) \quad (3.7)$$

where level q = p - 1, A_{pm} is the spontaneous transition probability, and $\Psi(x)$ and $\bar{\Phi}(x) = [\Psi(x)\, e^x]^{-1}$ are tabulated functions (Drawin (1969)). Substitution of approximate expressions for ΣA, f and $E_p - E_q$ appropriate for hydrogenic levels reduces equations (3.6) and (3.7) to the modified version of Griem's condition (equation (3.2)) discussed in section 3.2.

The essential feature to be noted in these generalised conditions is the dependence on the energy gap between adjacent levels. For complete LTE one then requires

that these conditions be satisfied for all levels, i.e. for all energy gaps in the ion level system. The most stringent condition arises from the largest energy gap, which in non-hydrogenic systems is not necessarily that between ground and first excited states, as it is in the hydrogenic case.

Then the condition for complete LTE may be written

$$N_e \geqslant 6.5 \times 10^{16} \frac{g_u}{g_\ell} \left(\frac{E_u - E_\ell}{E_H}\right)^3 \sqrt{\frac{kT_e}{E_H}} \Phi\left(\frac{E_u - E_\ell}{kT_e}\right) \qquad (3.8)$$

where u and ℓ denote respectively the upper and lower states separated by the largest energy gap.

This reduces to the hydrogenic case by putting u = 2 and ℓ = 1 and one obtains Griem's relation (equation (3.5)) apart from a slightly different numerical factor and multiplication by the "quantum mechanical correction" $\bar{\Phi}$ (x) which typically has values in the range 2 to 3 for x in the range 1 to 10.

The relation (3.8) has been evaluated for NI - NIV as well as HeI and HeII at kT_e = 3 eV, the maximum (optically allowed) energy gaps between adjacent states being obtained from the tables of Moore (1949); the values obtained are given in Table 3-1.

Table 3-1: Adjacent states with maximum (optically allowed) energy gaps (From Moore (1949)), and minimum N_e for LTE at kT_e = 3 eV.

Ion	ℓ	u	g_ℓ	g_u	$E_u - E_\ell$ (eV)	N_e (cm^{-3})
NI	$(1s^2 2s^2)\ 2p^3(^2P^o)$	$2p^2 3s(^4P)$	6	2	6.75	2.9×10^{15}
NII	$(1s^2)2s^2 2p^2(^1S)$	$2s2p^3(^3D^o)$	1	7	7.38	8.1×10^{16}
NIII	$(1s^2)2s^2 2p(^2P^o)$	$2s2p^2(^4P)$	4	2	7.07	5.0×10^{15}
NIV	$(1s^2)2s(^1S)$	$2s2p(^3P^o)$	1	3	8.33	5.1×10^{16}
HeI	$(1s)2p(^1P^o)$	$3s(^3S)$	3	3	1.50	4.6×10^{13}
HeII	$1s(^2S)$	$2p(^2P^o)$	2	2	40.8	2.6×10^{18}

Kulander (1965), using a model of 26 levels through all 8 ionization stages of nitrogen determined the minimum N_e for LTE in each ionization stage. This was taken as that value of N_e at which the "largest radiative rate" (for one of the assumed model levels in the ionization stage considered) becomes equal to the corresponding collisional rate, i.e. the Griem (1963) criterion for the level with the most stringent requirements. The values obtained are considerably higher than those calculated above from Drawin's criterion, presumably because of the crudeness of the assumed level structure; Kulander's values of N_e required for complete LTE in NI - NIV at $kT_e = 3$ eV are given in column 3 of Table 3-2.

House (1964) had earlier evaluated N_e LTE limits for nitrogen using only ground state and continuum for each ion; his values were at least an order of magnitude higher than those of Kulander, because of the omission of excited levels.

We now examine the possible application of the relations derived for hydrogenic ions to non-hydrogenic systems and nitrogen in particular.

Griem (1963) reasons that, since the oscillator strength cancelled out in the derivation of equation (3.5), this condition for complete LTE can be used for minimum N_e estimates in non-hydrogenic ions, "except for some uncertainties due to entirely different level structures in complex systems".

Further, Byron et al. (1962) argue that the dependence of the rate coefficients on the actual excitation energies is much stronger than their dependence on the specific wave functions of the excited states. One can thus obtain estimates by making level 2 in equation (3.5) the first excited level undergoing an optically allowed transition to the ground state. The N_e requirements thus obtained for NI to NIV are given in column 2 of Table 3-2.

Similarly, Wilson (1962) considers his relation, viz.

$$N_e \geqslant 6.0 \times 10^{12} E_\infty \sqrt{kT_e} \text{ cm}^{-3} \qquad (3.9)$$

to be applicable to a general ion. This generally gives more stringent conditions than Griem's relation; evaluation for NI - NIV yields the results given in column 4 of Table 3-2.

Cooper (1966) considers that Griem's relation should be applied "with care" to systems with low-lying resonance levels where partial LTE between ground and first excited states may exist without complete LTE in the ion; then Wilson's more stringent criterion should be applied to such systems.

The various minimum N_e estimates for NII and NIII are plotted against kT_e in the range 1-10 eV in Figure 3-1. These are:

Dr: Drawin's relation (equation (3.8)) in terms of the maximum energy gap (from Table 3-1)

Gr: Griem's relation (equation (3.5)) using the first excited level undergoing an optically allowed transition to ground

Ku: From Kulander's paper (1965)

Wi: Wilson's relation (equation (3.9)) in terms of the ionization energy.

Table 3-2: Minimum N_e for complete LTE in NI - NIV at kT_e = 3 eV from the criteria of Drawin (equation (3.8)), Griem (equation (3.5)), Kulander and Wilson (equation (3.9)).

Ion	Drawin	Griem	Kulander	Wilson
NI	2.9×10^{15}	1.9×10^{16}	3.0×10^{18}	3.1×10^{16}
NII	8.1×10^{16}	2.6×10^{16}	4.7×10^{17}	2.6×10^{17}
NIII	5.0×10^{15}	6.1×10^{15}	5.4×10^{17}	1.1×10^{18}
NIV	5.1×10^{16}	1.0×10^{16}	4.4×10^{18}	4.8×10^{18}

3.4 Effect of resonance line absorption

The effect of the absorption of the first resonance line in a hydrogenic ion on the minimum density requirement for complete LTE in that ion was considered by Griem (1963). At the densities required for LTE down to the first excited

Fig. 3-1 : Min. N_e for LTE

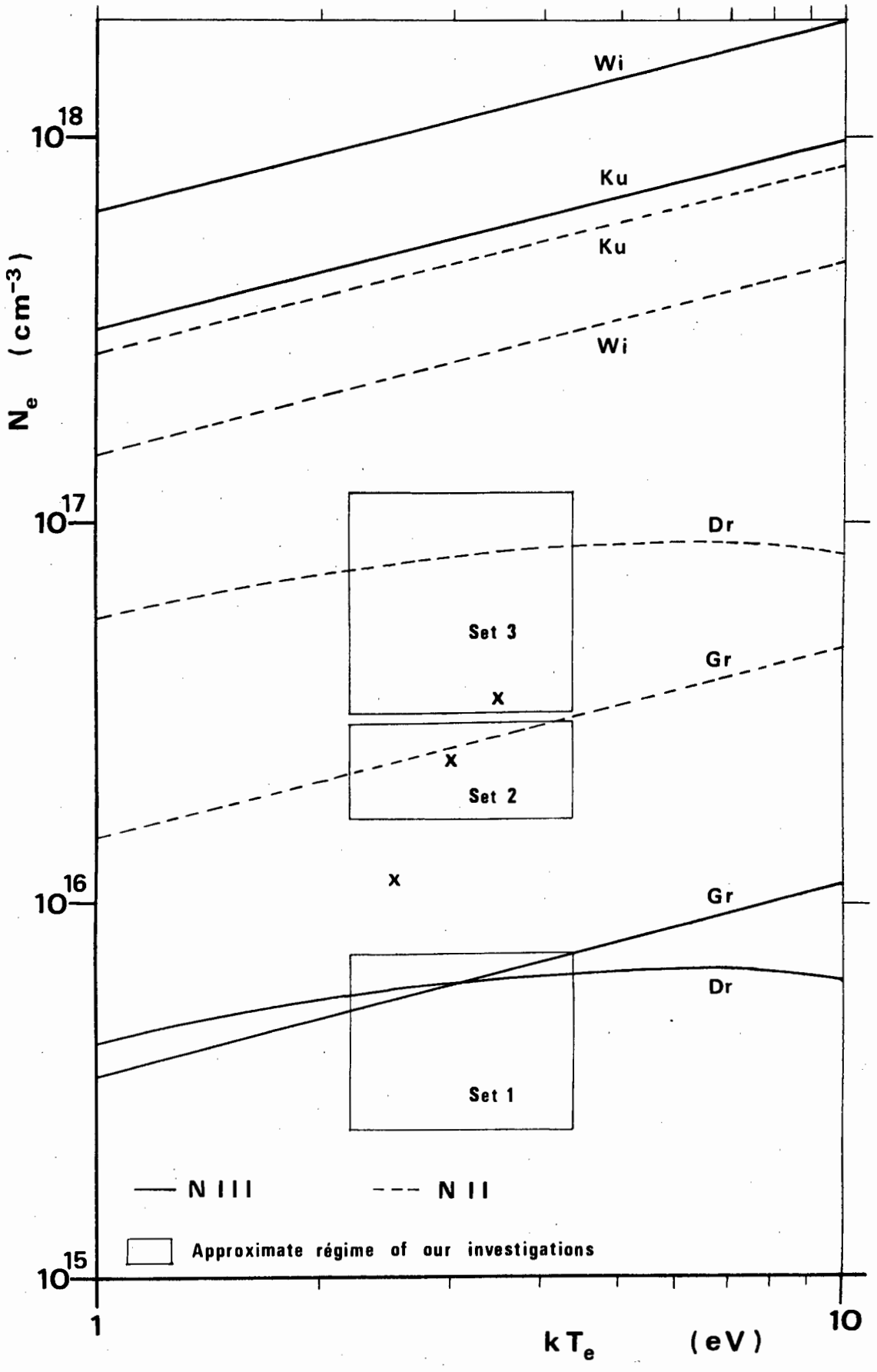

level, one may find that the radiative excitation rate of the ground state (which approximates the radiative population rate of the first excited state) balances the radiative decay rate of the first excited state. One must then consider radiative decay from higher states in the equilibrium of the ground state. Since this is an order of magnitude less important than that from the first excited state, the condition for partial LTE of the ground state (i.e. complete LTE) can be relaxed by the same factor.

Drawin (1969), however, estimates that such reductions should not be by more than a factor 2 or 3, while Fujimoto (1973) considers that at temperatures below about 1 eV, the N_e condition may be relaxed by as much as 2 orders of magnitude, but at higher temperatures no such relaxation is permitted.

We now consider the possibility of resonance line absorption in our nitrogen plasma. For this to be effective we require a sufficient number of absorbing ions in the path of the escaping radiation; Griem (1964) gives the following criterion for significant resonance absorption in terms of density of absorbing ions N_1^z (cm^{-3}) and plasma dimension d (cm):

$$N_1^z \, d \geq \frac{1.1 \times 10^{17}}{f \lambda} \sqrt{\frac{kT_e}{\mu}} \quad cm^{-2} \qquad (3.10)$$

where μ is the atomic mass number (14 for nitrogen) and f and λ (Å) the (absorption) oscillator strength and central wavelength respectively of the line. Kulander (1965) gives a relation equivalent to equation (3.10) apart from a smaller numerical factor of 9.3×10^{15}.

We now consider the evaluation of equation (3.10) for two important cases of NIII u.v. lines ending in the ground state, at $kT_e = 3$ eV:

(i) 374.2 Å, the strongest such line (f = 0.39 (Wiese et al. (1966))). Equation (3.10) yields

$$N_1^z \geq 7.0 \times 10^{13} \quad cm^{-3}$$

assuming a plasma dimension (radius) of 5 cm.

(ii) 452 Å, the upper level of which is the lower level of the lines 4097 and 4103 Å used in the intensity ratio measurements. Using $f = 0.047$ (Wiese et al., (1966)), we require $N_1^z \geq 4.8 \times 10^{14}\ cm^{-3}$ for significant absorption of 100, so that this condition is easily satisfied.

Kulander gives values of $1.1 \times 10^{13}\ cm^{-3}$ and $1.4 \times 10^{12}\ cm^{-3}$ for unit optical depth in NII and NIII respectively (using $d = 5$ cm), much less than the ground state densities above are of the same order as the total nitrogen density, so that it seems safe to assume complete optical thinness in our plasma.

(iii) the particle containment time t_{cont}

3.5 Supplementary conditions for LTE

The condition on N_e is a necessary but not sufficient condition for LTE. In addition one requires a number of other conditions to be satisfied, particularly with respect to the time variation of the plasma. In this final section we consider these criteria and show they are in all cases satisfied for our plasma.

(i) In order to assume a Maxwellian distribution of the free electrons (and therefore a meaningful electron temperature), we require that the condition on N_e for partial LTE of level p (equation (3.2)) be satisfied for at least one level p below the reduced ionization limit (Griem (1962, 1963)), i.e. for

$$p \leq \sqrt{\frac{E_\infty^z}{\Delta E_\infty^z}} = \sqrt{\frac{4\pi\varepsilon_0 \rho_D E_\infty^z}{ze}} \qquad (3.11)$$

where, the Debye radius $\rho_D = \sqrt{\frac{\varepsilon_0 kT_e}{e N_e}}$ m. (3.12)

(kT_e and E_∞^z in eV, N_e in m^{-3}, ε_0 and e in MKS units).

Thus one must rather consider the time required for the establishment

of LTE between these two states; in non-hydrogenic systems the equivalent would be the states separated by the largest energy gap (as the "weakest link" in the chain). This time τ_1 is given by the inverse of the ground state to first excited state collisional excitation rate for hydrogenic systems, i.e. by (Griem (1963)):

$$\tau_1 = \frac{1.15 \times 10^7}{f_{21} N_e} \quad \frac{E_2 - E_1}{E_H} \quad \sqrt{\frac{kT_e}{E_H}} \quad \exp\left(\frac{E_2 - E_1}{kT_e}\right) \text{ sec.} \qquad (3.15)$$

for complete ionization. (Drawin (1969) gives essentially the same relation, except that the exponential factor is replaced by $\Psi^{-1}\left(\frac{E_2 - E_1}{kT_e}\right)$ and the numerical factor is 0.89×10^7).

This yields times of the order of nanoseconds for NII and NIII, using the largest energy gap, at the minimum N_e required for LTE. Further, Griem (1963) considers that this may even be too stringent for decaying plasmas, since here recombination times will be extremely short and consideration should be given to radiative decay to the ground state in this case.

Because of the basic dependence on the energy gap, the relaxation times for higher excited states are generally smaller than that of the ground state. Since the lifetime of our plasma is of the order of several microseconds, it seems safe to assume an approximately stationary state; i.e. changes in electron temperature and density over the times of relaxation, etc. are small.

(iv) In addition to time-independence we have assumed spatial homogeneity of the plasma in considering the LTE criteria, and this assumption requires justification. We require that changes in electron temperature and density over distances of the order of the diffusion length λ_D of the ions with respect to collisional ionization be small, i.e. that such lengths be very much less than the plasma dimension. The most stringent condition is for ground state ions as they have the smallest cross-sections. Griem (1963, 1964) and Drawin (1969) give expressions for λ_D which on evaluation for NII and NIII

in our regime yield values of the order of 10^{-5} - 10^{-4} cm. Our plasma dimension (radius) is of the order of centimetres, so our assumption of approximate homogeneity is also seen to be justified.

CHAPTER 4

EXPERIMENTAL TECHNIQUES

In the first section of this chapter the apparatus used in our determinations and the experiments performed will be described. The following section considers the electron density measurements, and in the remainder of the chapter the theory yielding relations for the determination of electron temperature from measured line intensity ratios in the LTE and Semi-Corona regimes, the application of these relations, and the method of analysis of the data will be examined.

4.1 Experimental Arrangement

In order to obtain breakdown in the theta-pinch device in the density regime bordering on LTE, preionization of some kind is required. For our "low density" determinations (Set 1) ($N_e \sim 5 \times 10^{15}$ cm^{-3}; indicated in Fig. 3-1), r.f. preionization was used, with the gas already present in the theta-pinch tube at a certain initial pressure. For the "medium density" and "high density" (Sets 2 and 3 respectively) ($N_e \sim 10^{16} - 10^{17}$ cm^{-3}; also indicated in Fig. 3-1), a fast-acting electromagnetically-operated valve and coaxial plasma gun, to be described below, were used to project preionized gas into the centre of the theta-pinch.

4.1.1 The Plasma Gun

The fast-acting valve is a modified version of that developed at the Culham Laboratory and described by Hill and Montague (1966). The valve and gun are shown in through-section in Fig. 4-1, and the device operates as follows. The gas supply (N, N + He, H or H + He at a pressure (above atmospheric) of 5 p.s.i. for Set 2 (medium density) or 80 p.s.i. for Set 3 (high density)) is connected to the inlet A, filling the plenum B. A capacitor discharge through the coil N repels the circular steel and aluminium plate P against the spring S, lifting the valve V from its nylon seat T and admitting gas from

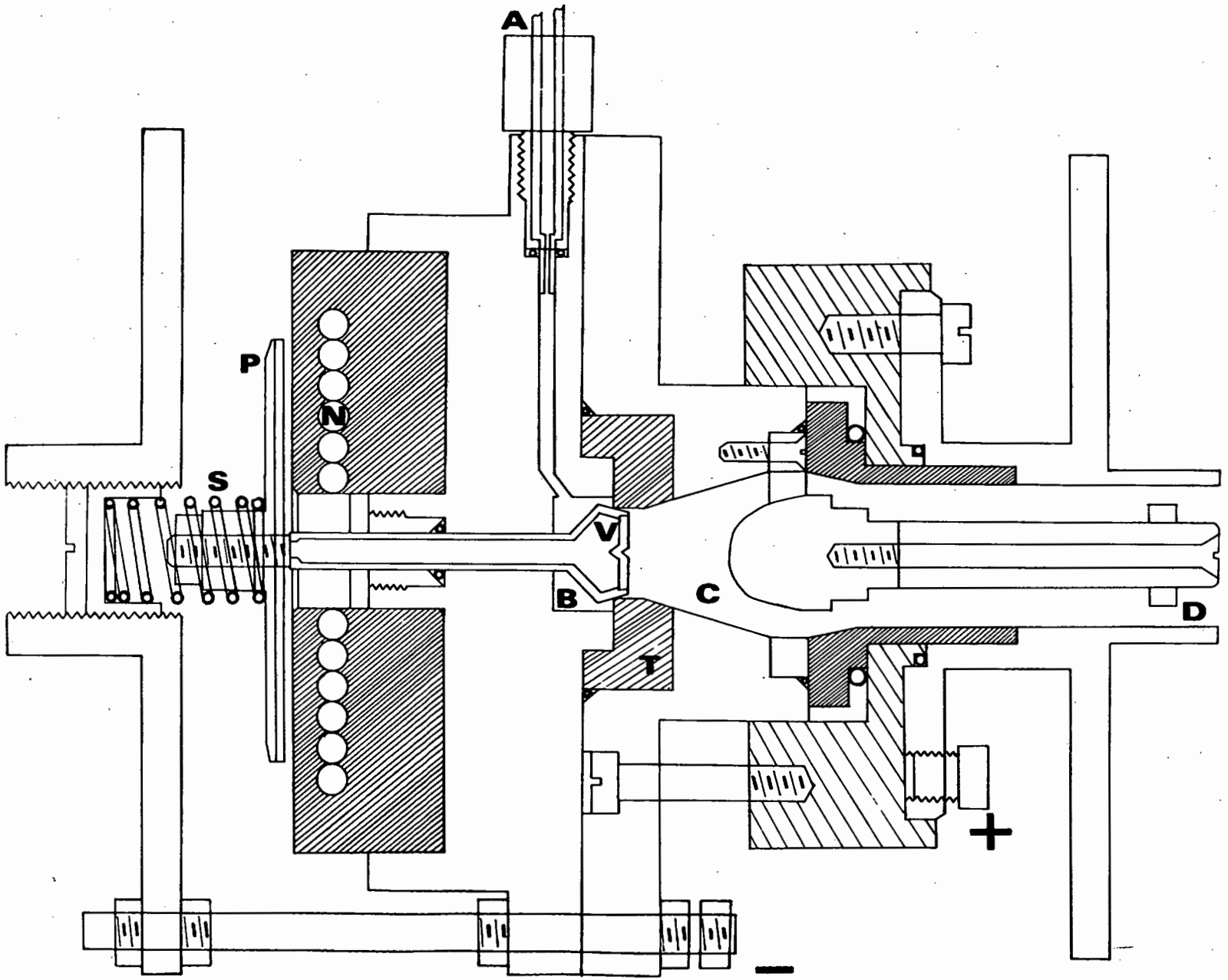

Fig. 4-1 : PLASMA GUN

the plenum into the region C. The gas then passes between the coaxial brass electrodes of the gun, and another capacitor discharge across the electrodes (connected as indicated by + and -) causes breakdown at D. The ionized gas is then emitted into the theta-pinch tube to the right.

4.1.2 The Experiments

Set 1 (Low density):

The gas (pure N or 50% N + He for the temperature measurements, pure H or 50% H + He for the density determinations) was let into the theta-pinch tube, originally evacuated below 0.01 mTorr, to a pressure of 10 mTorr. The main bank consisted of pairs of 8.5 μF, 20 kV capacitors which were charged in parallel through 500 kΩ resistors and discharged in series through the theta-pinch coil. Seven such pairs were connected in parallel. The 20 MHz r.f. preheater was switched on just before the main bank was fired. The discharge current had a peak value of 637 kA, a decrement of 0.5 and a period of 9 μsec; it was crowbarred at its first maximum (i.e. $2\frac{1}{4}$ μsec after the initiation of the discharge) to provide an approximately exponentially decaying current.

The light emitted from the centre of the theta-pinch was collimated and analysed using a Heath Scanning Monochromator (dispersion 20 Å/mm) and EMI6255B photomultiplier. The PM output was displayed with respect to time on a dual beam oscilloscope, together with the output from a coil current probe. The latter was displayed in order to fix the time origin of the intensity trace at the initiation of the discharge, as well as to check the shot to shot reproducibility of the main bank and crowbar. The oscilloscope traces were photographed and the intensity values at $\frac{1}{4}$ μsec intervals for $4\frac{1}{2}$ μsec from the start of the discharge extracted.

In order to reduce intensities differing by as much as two orders of magnitude to a standard range on the oscilloscope (between 4 and 8 V), the photomultiplier EHT supply voltage was used as scaling factor. The PM output with respect to supply voltage is given in Fig. 4-2(a); settings of from 800 V for

the strongest lines to 1400 V for the weakest were used. The measured intensity also has to be corrected for the PM response at different wavelenths, which is shown in Fig. 4-2(b). The raw intensity data were read into the computer programs (to be described later) and multiplied by the "scale factor" and "PM factor" therein.

Sets 2 and 3 (Medium and high density):
The gas supply (at 5 and 80 p.s.i. respectively) was connected to the valve inlet, with the pinch tube evacuated as before. The main bank was again charged to 12 kV, and in addition two similar 8.5 μF capacitors, providing energy for the valve and gun, were also charged to 12 kV. The first capacitor was discharged through the valve coil and the second across the gun about 400 μsec later; the main bank was fired 38 μsec after the gun, when the front of the preionized plasma from the gun reached the far end of the theta-pinch coil. The current was again crowbarred and the intensities extracted as before.

A block diagram of the circuitry is given in Fig. 4-3 and the detailed apparatus parameters are given in Table 4-1.

4.1.3 Lines Observed

In our temperature regime NII and NIII are expected to be the dominant ionic species of nitrogen present. The NII and NIII lines given in Table 4-2 were selected for intensity measurements on the basis of the following requirements:

(i) wavelength within the range of the photomultiplier (see Fig. 4-2(b));
(ii) sufficiently large observed intensity (at least a factor 3 above background);
(iii) sufficiently large oscillator strength (generally > 0.1);
(iv) sufficient separation from neighbouring lines (generally $> 4\text{Å}$).

Also given in Table 4-2 are the HeI and HeII lines observed in the cases where the N + He mixture was used (selected according to the same criteria).

Fig. 4-2

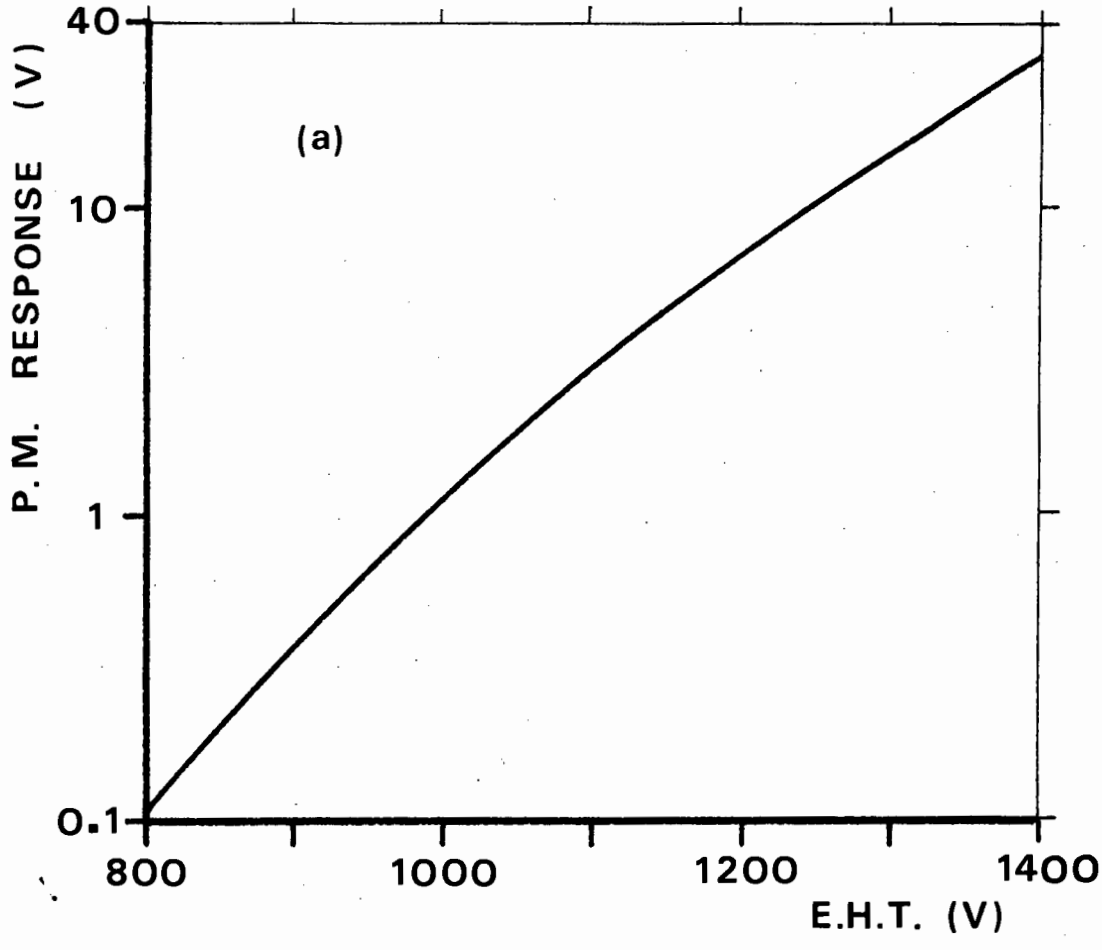
40
10
1
0.1
P.M. RESPONSE (V)
(a)
800
1000
1200
1400
E.H.T. (V)

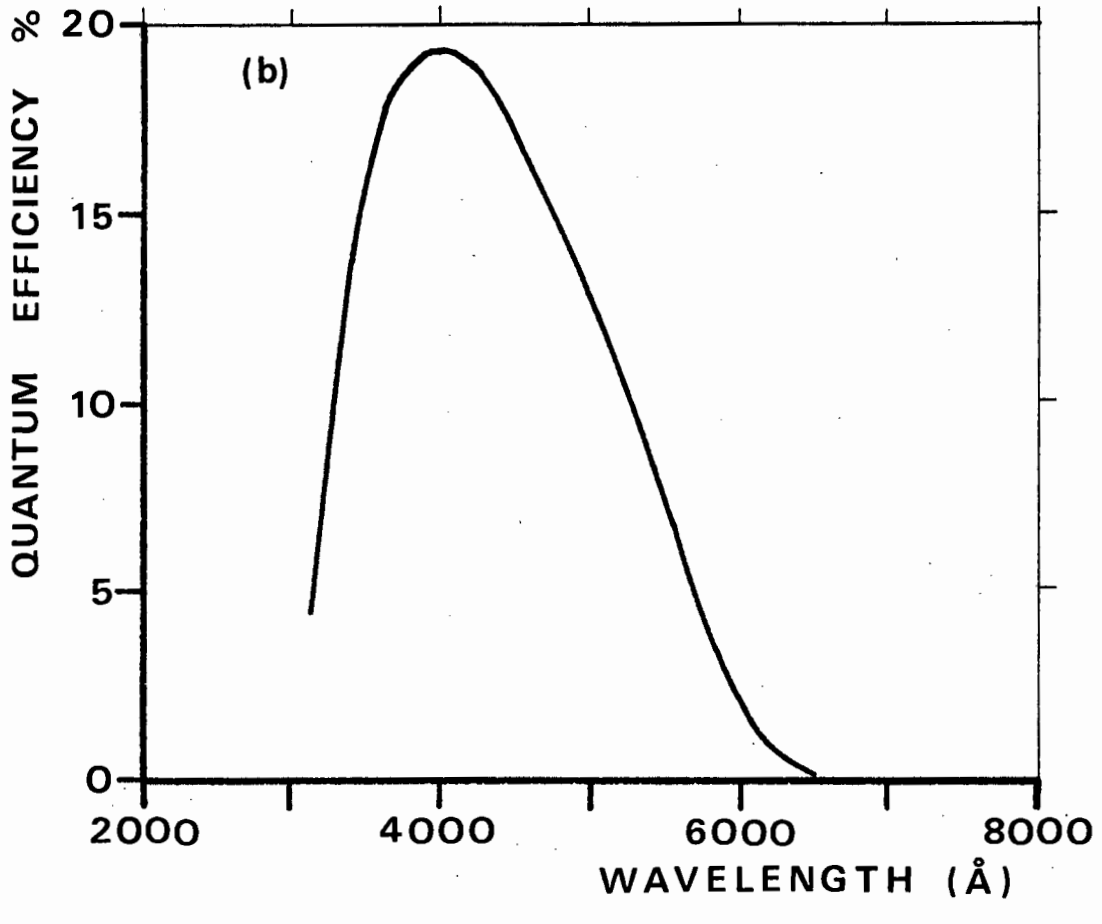
20
15
10
5
0
QUANTUM EFFICIENCY %
(b)
2000
4000
6000
8000
WAVELENGTH (Å)

Fig. 4-3 : CIRCUITRY

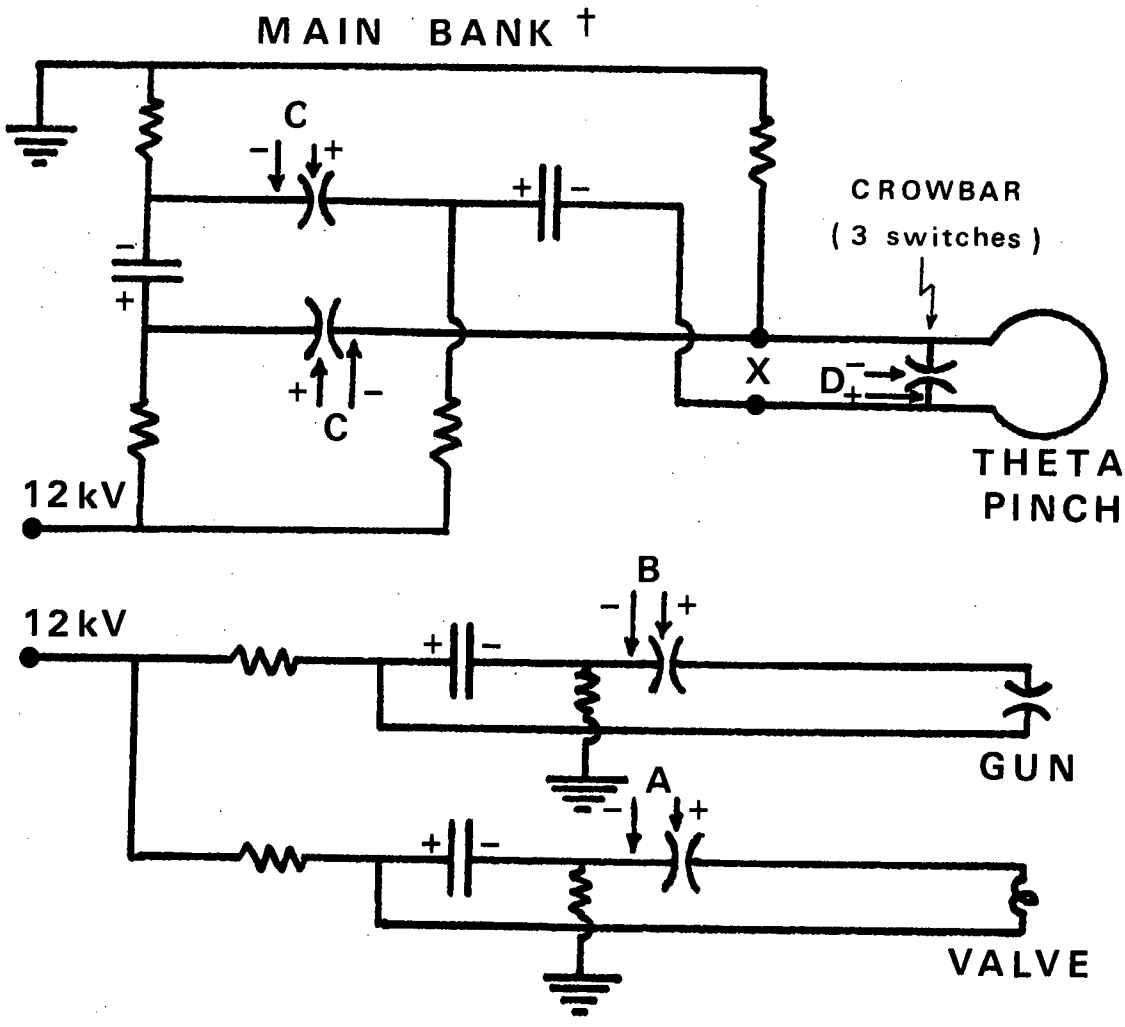

Triggering (schematic) :

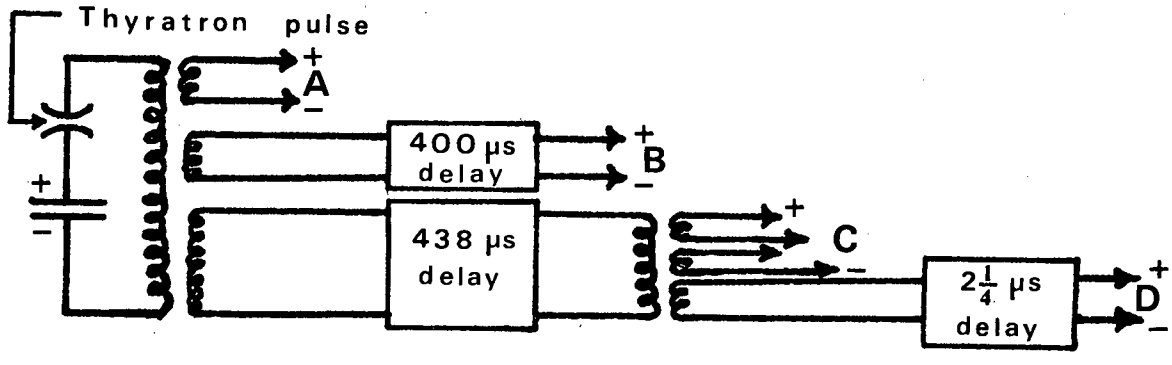

all 8.5 μF , 20 kV

all 500 kΩ

† 7 similar circuits in parallel at X

The electron density determinations in H and H + He from measured widths of the lines $H\beta$ and $H\gamma$ are described in the next section.

Table 4-1: Apparatus parameters

(a) Circuit parameters

	Valve	Gun	θ-Pinch
Capacitance (μF)	8.5	8.5	29.75
Voltage (kV)	12	12	12
Peak current (kA)	80	80	637
Energy (kJ)	0.6	0.6	8.6
Circuit inductance (nH)	700	47	40
Capacitor inductance (nH)	91	91	26
Switch inductance (nH)	56	56	16
Discharge period (μs)	8	8	9

Delay times: Valve-Gun: 400 μsec
Gun-Main bank 38 μsec
Bank-Crowbar: 2.25 μsec

(b) Theta pinch dimensions

Coil length: 32 cm
Tube length: 74 cm
Tube diameter: 10 cm
Gun barrel diameter: 2.4 cm

(c) Monochromator

Dispersion: 20 Å/mm
Entrance slit width: 10 μ
Exit slit width: 100μ ≡ 2 Å or 50μ

4.2 Electron Density Determinations

4.2.1 Theoretical background

Under conditions where Stark broadening is the dominant line broadening mechanism in a plasma, the electron density may be most conveniently

TABLE 4-2 : LINES OBSERVED

WAVELENGTH LAMBDA (A) , OSCILLATOR STRENGTH F , LOWER LEVEL STATISTICAL WEIGHT G , UPPER LEVEL ENERGY E (CM-1) , AND EFFECTIVE PRINCIPAL QUANTUM NUMBER OF UPPER LEVEL N*

ION	NO.	LAMBDA	F	G	E	N*
N II	1	3919.01	.231	3	190121	3.00
	2	4145.76	.117	7	229840	7.02
	3	4176.16	.800	5	211031	3.98
	4	4227.75	.171	5	197859	3.28
	5	4447.03	.587 A	3	187092	2.91
	6	4601.48	.133 A	3	170667	2.54
	7	4613.87	.080 A	3	170609	2.54
	8	4630.54	.269	5	170667	2.54
	9	4803.27	.108	7	187493	2.93
N III	1	3754.62	.088	4	314224	3.80
	2	4097.31	.486	2	245702	2.68
	3	4103.37	.244	2	245666	2.68
	4	4379.09	.788 B	8	342809	4.98
	5	4514.89	.286	6	309857	3.68
	6	4518.18	.178	2	309663	3.68
	7	4634.16	.428 A	2	267230	2.92
HE I	1	3888.65	.064	3	185565	2.93
	2	4471.50	.125	9	191445	4.00
	3	5875.70	.609	9	186102	3.00
HE II	1	4685.68	1.018	10	411452	4.00
	2	5411.52	.058 C	14	429923	6.99

ALL VALUES FROM WIESE ET.AL.(1966) EXCEPT : A - FROM GRIEM (1964) ; B - FROM ALLEN (1955) ; C - CALCULATED FROM THE TABULATIONS OF GREEN ET.AL.(1957).

determined from measurements of the half-widths of isolated spectral lines. Stark broadening dominates at moderate temperatures and densities (including our plasma regime); Doppler (thermal) broadening becomes dominant only at higher temperatures (approaching 100 eV) and lower densities ($<10^{13}$ cm^{-3}), while natural broadening is negligible even compared to Doppler broadening for light ions with $Z < 10$ (Cooper (1966)).

After Griem (1964), one may write the relationship between electron density N_e (cm^{-3}) and full Stark width $\Delta\lambda_s$ (Å) as:

$$N_e = C(N_e, T_e)\,\Delta\lambda_s^{3/2} \qquad (4.1)$$

where the coefficient $C(N_e, T_e)$ is a weak function of electron density and temperature; its values, typically 3×10^{14} cm^{-3} Å$^{-3/2}$ for the hydrogen Balmer lines $H\beta$ and $H\gamma$, are given by Griem (1964).

These lines were used in our measurements of N_e because:
(i) their wavelengths (4861 Å and 4340 Å respectively) lie in the PM range;
(ii) their large widths (>10 Å for $N_e > 10^{16}$ cm^{-3}) make for easy and reliable measurements (particularly using instruments with limited resolution);
(iii) the coefficients for these lines are well established and readily available.

4.2.2 Experimental N_e measurements

H and 50% H + He were used at the same initial pressures as the N and N + He in the three sets of experiments. The two lines were scanned in suitable wavelength steps with a small monochromator slit width (8 microns). The resulting intensity versus wavelength plots for each time (every $\frac{1}{4}$ μsec for $4\frac{1}{2}$ μsec) yielded the FWHM $\Delta\lambda$ and the N_e values were obtained from the graphs given in Fig. 4-4(a).

The N_e values obtained from the two lines agreed with each other within the theoretical and experimental error limits of 10%, and the mean of the two was used. The results (N_e versus time) are plotted in Fig. 4-4(b)

Fig. 4-4

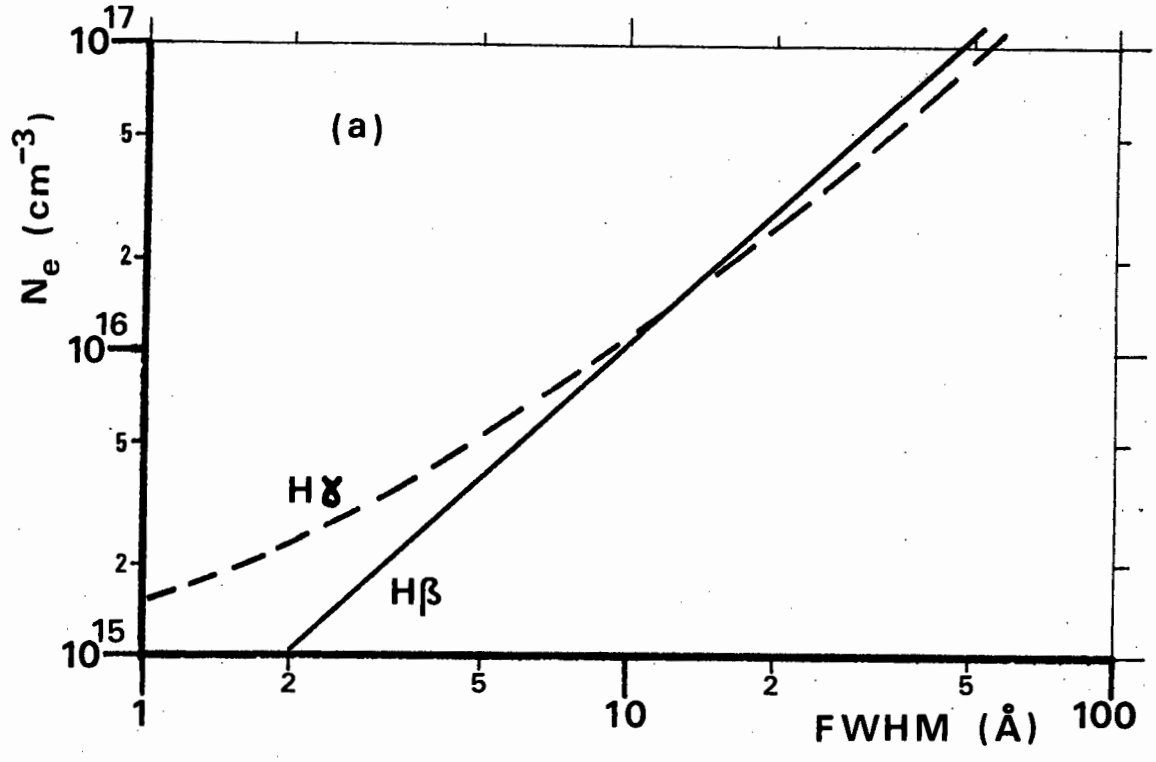
(a)
N_e (cm^{-3})
10^{17}
5
2
10^{16}
5
2
10^{15}
Hγ
Hβ
1
2
5
10
2
5
100
FWHM (Å)

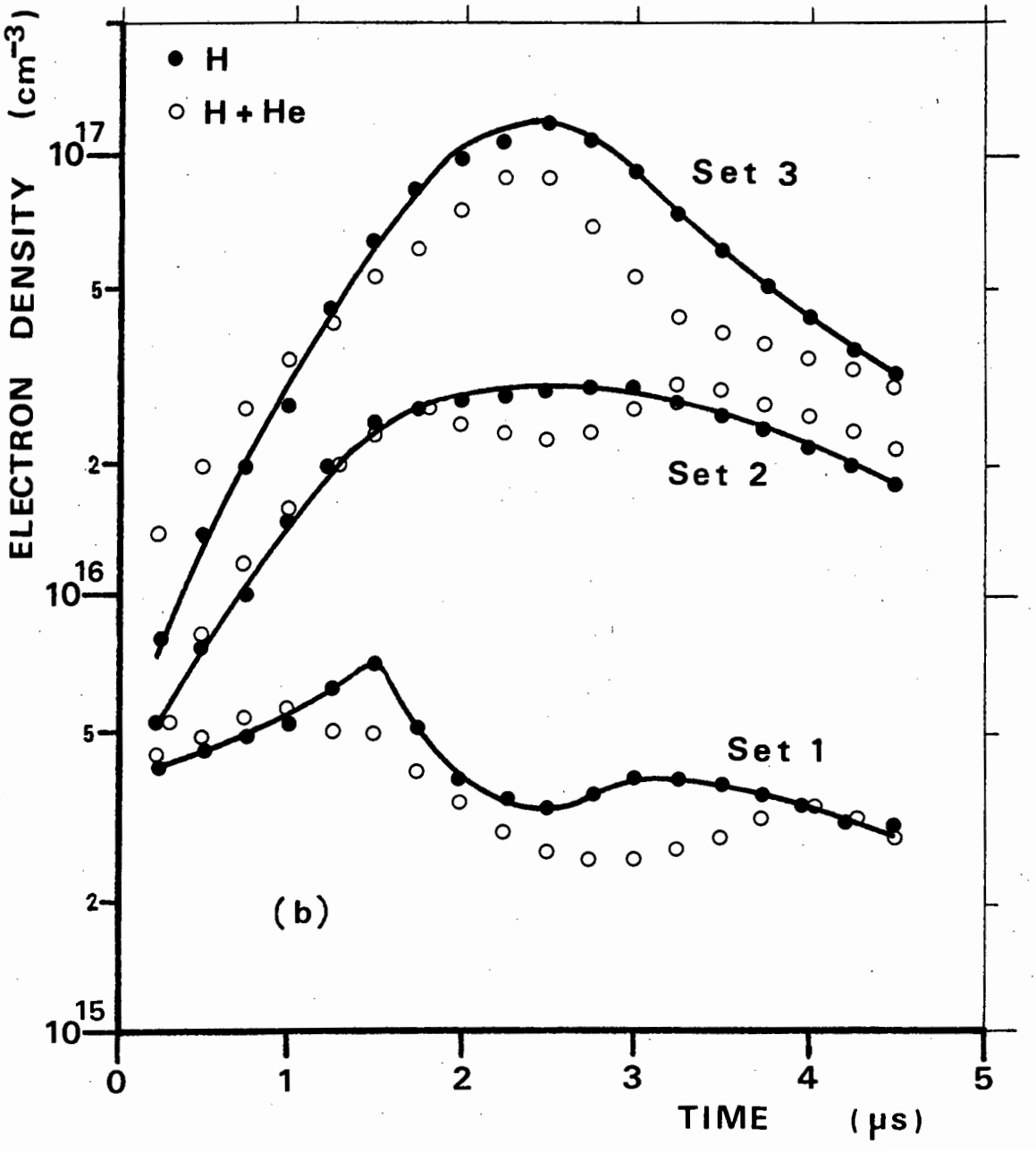
ELECTRON DENSITY (cm^{-3})
● H
○ H + He
10^{17}
5
2
10^{16}
5
2
10^{15}
Set 3
Set 2
Set 1
(b)
0
1
2
3
4
5
TIME (μs)

for the three sets (low, medium and high density) using both H and H + He. It can be seen that in each set N_e is very nearly the same for the two cases. This is to be expected because He is predominantly singly ionized in our temperature domain, and the volume of gas (and therefore the number of atoms) admitted (dependent predominantly on the initial pressure) should be approximately the same.

In order to obtain the electron densities in the nitrogen plasmas half-width measurements should be carried out in H + N mixtures. However, reliable results are ruled out by the presence of a number of NII and NIII lines in the wavelength region of the two Balmer lines; in particular there is a strong NIII line at 4861.3 Å (the central wavelength of $H\beta$). Measurements of the half-widths of nitrogen lines could not give useful results because (i) their theoretical profiles are uncertain; (ii) the widths are smaller and their variation with N_e is much less sensitive than the hydrogen lines; (iii) experimental measurements of such widths would have large uncertainties.

We therefore assume the electron density in the N and N+He plasmas to be the same as that measured in the H and H + He plasmas, i.e. as given in Fig. 4-4(b). This is justified as long as the same quantity of gas (number of atoms) is admitted and NII is the dominant ionic species of nitrogen present; if NII and NIII are present in approximately equal proportions the assumption will still be correct within a factor 1.5. Rough measurements on $H\beta$ and $H\gamma$ in N + H mixtures indicated this to be true.

4.3 Temperature Determination from Line Intensity Ratios

There are a number of spectroscopic methods available for the determination of the electron temperature in a plasma in the LTE or Semi-Corona regimes. These include:

(i) intensity ratios of lines from the same element and ionization stage;

(ii) intensity ratios of lines from successive ionization stages;

(iii) line-to-continuum intensity ratios;

(iv) relative continuum intensities.

Method (ii) is used here for the following reasons:

(a) continuum intensity measurements are usually subject to large uncertainties;

(b) methods (iii) and (iv) can only be used for pure gases; we require to measure kT_e in gaseous mixtures;

(c) the sensitivity to temperature of a line intensity ratio depends on the energy difference between the upper states of the lines; these differences are enhanced in method (ii) over method (i) by the ionization energy of the lower stage.

The two relations for the intensity ratio of lines from successive ionization stages in terms of kT_e applicable in the LTE and Semi-Corona regimes will now be presented; these relations are given by Griem (1964) and formal derivations are given by Hey (1970).

The intensity I^z_{pm} of an emitted line (transition m → p, ionization stage z) depends on the population N^z_m of the upper level m and the transition probability A^z_{pm} according to the relation

$$I^z_{pm} = N^z_m \, A^z_{pm} \, h\nu^z_{pm} \tag{4.2}$$

The ratio of this intensity to that of the transition n → q (ionization stage z - 1) is therefore given by

$$\frac{I^z_{pm}}{I^{z-1}_{qn}} = \frac{N^z_m \, A^z_{pm} \, \nu^z_{pm}}{N^{z-1}_n \, A^{z-1}_{qn} \, \nu^{z-1}_{qn}} \tag{4.3}$$

or in terms of the absorption oscillator strength

$$f^z_{mp} = \frac{c \, g^z_m \, A^z_{pm}}{8\pi^2 r_o (\nu^z_{pm})^2 \, g^z_p} \tag{4.4}$$

(where g^z_m, g^z_p are the statistical weights, r_o the classical electron radius) and wavelength λ^z_{pm} by

$$\frac{I^z_{pm}}{I^{z-1}_{qn}} = \frac{N^z_m}{N^{z-1}_n} \frac{g^z_p}{g^{z-1}_q} \frac{g^{z-1}_n}{g^z_m} \frac{f^z_{mp}}{f^{z-1}_{nq}} \left(\frac{\lambda^{z-1}_{nq}}{\lambda^z_{mp}} \right)^3 \qquad (4.5)$$

The different relations for the intensity ratio in the LTE and Semi-Corona cases arise from the use of different expressions for the relative level populations N^z_m, N^{z-1}_n in the two cases.

4.3.1 LTE Case

Here the population of the upper level m in ionization stage z is given relative to the ground state population N^z_1 by the Boltzmann equation

$$\frac{N^z_m}{N^z_1} = \frac{g^z_m}{g^z_1} \exp - \frac{\left(E^z_m - E^z_1\right)}{kT_e} \qquad (4.6)$$

and the population of the upper level n in the lower ionization stage z-1 is given relative to N^z_1 by the Saha equation

$$\frac{N^z_1 N_e}{N^{z-1}_n} = 2 \frac{g^z_1}{g^{z-1}_n} \left(\frac{m_e kT_e}{2\pi\hbar^2} \right)^{3/2} \exp - \frac{\left(E^{z-1}_\infty - E^{z-1}_n + E^{z-1}_1\right)}{kT_e} \qquad (4.7)$$

where E^{z-1}_∞ is the ionization energy, m_e the electron mass.

We thus assume that the higher ionization stage z is in complete LTE (allowing the use of the Boltzmann equation) and that the upper level n of the line in the lower ionization stage z-1 is above the thermal limit n_t, i.e. this level is in partial LTE (allowing the use of the Saha equation to link its population to that of the continuum).

The ratio $\frac{N^z_m}{N^{z-1}_n}$ may then be obtained from equations (4.6) and (4.7); substituting in (4.5) and simplifying, we obtain

$$\boxed{\frac{I'}{I} = \frac{2f'g'\lambda'^3}{N_e f g \lambda^3} \left(\frac{m_e kT_e}{2\pi\hbar^2} \right)^{3/2} \exp - \frac{\left(E' + E_\infty - E\right)}{kT_e}} \qquad (4.8)$$

where primed and unprimed quantities refer to ionization stages z and z-1 respectively; g, g' are the statistical weights of the lower levels involved in the transitions; $E = E_n^{z-1} - E_1^{z-1}$ and $E' = E_m^z - E_1^z$ are the positive excitation energies of the upper levels relative to the respective ground states.

4.3.2 Semi-Corona case

Here we assume that the upper levels m and n are above the respective thermal limits, so that they are in each case in Saha equilibrium with the ground state of the next highest ionization stage; i.e. N_n^{z-1} is again given by (4.7), and N_m^z is similarly given relative to N_1^{z+1}. Since the Saha equation is used in both cases, N_e cancels out, and the ratio of upper level populations is given by

$$\frac{N_m^z}{N_n^{z-1}} = \frac{N_1^{z+1}}{N_1^z} \frac{g_1^z}{g_1^{z+1}} \frac{g_m^z}{g_n^{z-1}} \exp \frac{E_\infty^z - E_m^z - E_\infty^{z-1} + E_n^{z-1}}{kT_e} \qquad (4.9)$$

We now assume (as in Chapter 2) that the ground state populations N_1^z, N_1^{z+1} are approximately equal to the total ion populations N_a^z, N_a^{z+1}; i.e. that the total excited state populations $\sum_{p=2}^{p\,max} N_p^z$, $\sum_{p=2}^{p\,max} N_p^{z+1}$ are negligible compared to N_1^z, N_1^{z+1}. This is justified (Bates et. al. (1962)) if the mean thermal energy of the ions is considerably less than the first excitation energy; this is valid in our case. N_a^z and N_a^{z+1} are then related by the Corona relation (Woolley and Allen (1948)); i.e. we have

$$\frac{N_1^{z+1}}{N_1^z} \doteq \frac{N_a^{z+1}}{N_a^z} = \frac{S^z}{\alpha^{z+1}} \qquad (4.10)$$

where S^z, α^{z+1} are the (collisional-radiative) ionization and recombination coefficients for $z \rightleftharpoons z+1$.

Substituting (4.10) into (4.9) and the latter into (4.5) we obtain, after simplification:

$$\frac{I'}{I} = \frac{S'}{\alpha''} \frac{g_1'}{g_1''} \frac{f'g'\lambda^3}{f\,g\,\lambda'^3} \exp\left(\frac{E_\infty' - E' - E_\infty + E}{kT_e}\right) \qquad (4.11)$$

where unprimed, primed and doubly primed quantities refer to ionization stages z-1, z and z+1 respectively; g, g', E, E' have the same meanings as before.

4.4 Application of the Relations

4.4.1 LTE case

Utilization of the LTE intensity ratio relation (4.8) for temperature determination is a fairly straightforward procedure. The experimentally determined value of N_e and tabulated values of the energies E, E', oscillator strengths f, f' and statistical weights g, g' for two particular lines are inserted. The electron temperature kT_e is used as a trial parameter, incremented in suitable steps, and the resultant trial intensity ratios are computed. The value of kT_e which gives the calculated ratio closest to the experimental value is then taken as the correct one. Similar computations for a number of line pairs will then enable one to obtain a fairly reliable mean value of kT_e, with associated statistical spread; all line pairs should, of course, ideally yield the same temperature. In our case the use of seven NIII and nine NII lines provided 63 ratios. The appropriate values of λ, E, f and g for the lines used, taken from the tabulations of Wiese et al. (1966) with a few exceptions, are given in Table 4-2. kT_e was incremented in 0.2 eV steps from 1 to 7 eV; for each line pair the kT_e solution was taken as that value at which the difference between the calculated and measured intensity ratios was a minimum. A mean of the 63 values, with associated statistical deviation, was then obtained at each time (every $\frac{1}{4}$ μsec for $4\frac{1}{2}$ μsec). The computer program RLTE used is given in the Appendix.

4.4.2 Semi-Corona Case

The use of equation (4.11) to determine kT_e is complicated by the fact that the coefficients S and α are very poorly known for non-hydrogenic ions (as discussed in Chapter 2). Therefore the ratio S/α and kT_e were simultaneously determined by a type of "best fit by least squares" technique, described below, from the 63 experimental intensity ratios.

Equation (4.11) was written as an explicit relation for S/α, i.e.

$$\frac{S'}{\alpha''} = \frac{I'}{I} \frac{g_1''}{g_1'} \frac{f g \lambda'^3}{f' g' \lambda^3} \exp\left(\frac{-E_\infty' - E' - E_\infty + E}{kT_e}\right) \quad (4.12)$$

and the tabulated f's, g's and E's and measured I's for a particular line pair inserted. kT_e was again used as a trial parameter in suitable increments (0.25 eV from 1 to 8 eV) and the corresponding values of S/α computed. This was repeated for all 63 NIII - NII line pairs, so that a series of tabulated "plots" of S/α versus kT_e were obtained. Ideally these plots for the different line pairs should give a family of curves with different slopes, concurrent at a point indicating the true values of the two parameters. In practice, because of uncertainties in the intensities and oscillator strengths, and because in some cases the upper level of the transition may be close to or actually below the thermal limit, there will be convergence but not actual concurrence of the curves.

The true value of kT_e can then be taken as that value of the trial parameter at which the minimum spread in the S/α values from individual line pairs occurs, and the true value of S/α can be taken as the mean of the values at that particular kT_e.

Now the incorporation of all 63 line pairs in one "family" will only give one value of kT_e, with no estimate of the uncertainty. Thus the line pairs were analysed as follows: Two NIII lines were taken at a time and combined with all nine NII lines (i.e. the curves for 18 line pairs constituted one family).

The value of kT_e at which the minimum percentage standard deviation amongst the S/α values occurred, and the mean of the 18 values at that kT_e (i.e. the "true" kT_e and S/α) were obtained.

This was repeated for each possible combination of two NIII lines (7 lines yielded 21 combinations of 2), and the means of the resulting 21 values of S/α and kT_e, with associated standard deviations, were obtained; these were taken as the "final solutions" at each time. The computer program RCOR used for this analysis is given in the Appendix.

NUMERICAL RESULTS

Table 5-1:

(a)	Low density N
(b)	Low density N + He
(c)	Medium density N
(d)	Medium density N + He
(e)	High density N
(f)	High density N + He

TABLE 5-1 (A)

EXPERIMENT NO. : 9 DENSITY SET : LOW GAS : N

TIME (US)	NE (CM-3)	LTE KT (EV)	S-C KT (EV)	S/ALPHA
.25	4.2+15	2.55 ± .04	3.97 ± .66	7.88-02 ± .23-01
.50	4.5+15	2.50 ± .03	1.77 ± .28	2.41-02 ± .81-01
.75	4.8+15	2.47 ± .03	2.77 ± .36	2.21-02 ± .49-02
1.00	5.3+15	2.62 ± .02	2.90 ± .18	4.14-02 ± .71-02
1.25	6.2+15	2.79 ± .02	3.57 ± .19	1.52-01 ± .18-01
1.50	7.4+15	2.84 ± .02	3.77 ± .19	2.06-01 ± .21-01
1.75	5.0+15	2.85 ± .02	3.27 ± .15	2.45-01 ± .24-01
2.00	3.8+15	2.82 ± .02	3.80 ± .11	3.41-01 ± .21-01
2.25	3.4+15	2.72 ± .02	3.90 ± .29	2.26-01 ± .39-01
2.50	3.3+15	2.68 ± .02	3.72 ± .28	1.69-01 ± .30-01
2.75	3.5+15	2.63 ± .03	4.20 ± .38	1.49-01 ± .28-01
3.00	3.8+15	2.58 ± .03	4.12 ± .33	9.64-02 ± .18-01
3.25	3.8+15	2.53 ± .03	3.72 ± .38	5.88-02 ± .12-01
3.50	3.7+15	2.40 ± .03	3.40 ± .33	2.51-02 ± .58-02
3.75	3.5+15	2.31 ± .02	3.02 ± .27	1.10-02 ± .24-02
4.00	3.3+15	2.24 ± .03	2.97 ± .37	8.74-03 ± .23-02
4.25	3.1+15	2.20 ± .04	2.85 ± .41	8.02-03 ± .24-02
4.50	2.9+15	2.17 ± .04	2.62 ± .17	8.25-03 ± .26-02

TABLE 5-1 (B)

EXPERIMENT NO. : 10 DENSITY SET : LOW GAS : N+HE

TIME (US)	NE (CM-3)	LTE KT (EV)	S-C KT (EV)	S/ALPHA
.25	4.2+15	2.61 ± .03	3.33 ± .36	9.16-02 ± .20-01
.50	4.5+15	2.59 ± .03	4.23 ± .34	7.97-02 ± .14-01
.75	4.8+15	2.55 ± .03	4.60 ± .31	7.98-02 ± .12-01
1.00	5.3+15	2.66 ± .03	4.78 ± .40	1.38-01 ± .20-01
1.25	6.2+15	2.81 ± .02	3.48 ± .16	1.69-01 ± .18-01
1.50	7.4+15	2.91 ± .02	3.45 ± .28	2.50-01 ± .34-01
1.75	5.0+15	2.86 ± .02	3.68 ± .25	3.19-01 ± .36-01
2.00	3.8+15	2.80 ± .02	3.52 ± .18	2.69-01 ± .29-01
2.25	3.4+15	2.72 ± .02	3.62 ± .15	1.99-01 ± .18-01
2.50	3.3+15	2.66 ± .02	3.92 ± .16	1.55-01 ± .11-01
2.75	3.5+15	2.60 ± .02	4.03 ± .16	1.06-01 ± .74-02
3.00	3.8+15	2.54 ± .02	3.83 ± .14	6.63-02 ± .45-02
3.25	3.8+15	2.47 ± .01	3.68 ± .14	3.82-02 ± .37-02
3.50	3.7+15	2.40 ± .02	3.55 ± .12	2.25-02 ± .22-02
3.75	3.5+15	2.33 ± .02	3.17 ± .10	1.28-02 ± .15-02
4.00	3.3+15	2.29 ± .02	2.90 ± .11	7.86-03 ± .96-03
4.25	3.1+15	2.27 ± .02	2.60 ± .10	6.80-03 ± .85-03
4.50	2.9+15	2.26 ± .02	2.45 ± .08	5.42-03 ± .55-03

TABLE 5-1 (C)

EXPERIMENT NO. : 20 DENSITY SET : MED GAS : N

TIME (US)	NE (CM-3)	LTE KT (EV)	S-C KT (EV)	S/ALPHA
.25	5.2+15	3.01 ± .03	3.18 ± .31	9.51-01 ± .23+00
.50	7.7+15	2.89 ± .03	2.95 ± .24	4.01-01 ± .12+00
.75	1.0+16	2.68 ± .03	2.13 ± .12	6.26-02 ± .15-01
1.00	1.5+16	2.75 ± .02	2.57 ± .22	5.08-02 ± .12-01
1.25	2.0+16	2.94 ± .02	2.09 ± .12	5.72-02 ± .12-01
1.50	2.5+16	3.18 ± .02	2.53 ± .16	2.32-01 ± .34-01
1.75	2.7+16	3.30 ± .01	3.11 ± .12	4.24-01 ± .25-01
2.00	2.8+16	3.27 ± .01	3.09 ± .09	3.67-01 ± .23-01
2.25	2.9+16	3.35 ± .01	2.97 ± .09	4.55-01 ± .33-01
2.50	3.0+16	3.40 ± .02	3.30 ± .12	6.00-01 ± .57-01
2.75	3.1+16	3.32 ± .02	3.53 ± .14	5.13-01 ± .37-01
3.00	3.0+16	3.22 ± .01	3.33 ± .09	2.82-01 ± .15-01
3.25	2.8+16	3.07 ± .01	3.18 ± .06	1.46-01 ± .47-02
3.50	2.6+16	3.01 ± .01	2.89 ± .06	9.85-02 ± .44-02
3.75	2.4+16	2.88 ± .01	2.78 ± .03	4.96-02 ± .75-03
4.00	2.2+16	2.80 ± .01	2.68 ± .04	3.08-02 ± .12-02
4.25	2.0+16	2.68 ± .01	2.70 ± .05	1.82-02 ± .92-03
4.50	1.8+16	2.60 ± .01	2.49 ± .02	9.70-03 ± .34-03

TABLE 5-1 (D)

EXPERIMENT NO. : 17 DENSITY SET : MED GAS : N+HE

TIME (US)	NE (CM-3)	LTE KT (EV)	S-C KT (EV)	S/ALPHA
.25	5.2+15	2.68 * .02	1.62 * .10	4.25-02 * .77-02
.50	7.7+15	2.72 * .03	1.67 * .10	4.04-02 * .76-02
.75	1.0+16	2.77 * .02	1.65 * .12	3.01-02 * .43-02
1.00	1.5+16	2.86 * .02	1.97 * .15	3.60-02 * .50-02
1.25	2.0+16	3.04 * .02	2.13 * .16	8.23-02 * .17-01
1.50	2.5+16	3.25 * .02	2.40 * .21	2.31-01 * .43-01
1.75	2.7+16	3.30 * .03	1.87 * .13	1.88-01 * .38-01
2.00	2.8+16	3.36 * .03	2.17 * .16	2.54-01 * .48-01
2.25	2.9+16	3.45 * .02	2.70 * .20	5.72-01 * .11+00
2.50	3.0+16	3.41 * .02	3.02 * .17	5.01-01 * .55-01
2.75	3.1+16	3.35 * .02	3.17 * .13	3.59-01 * .30-01
3.00	3.0+16	3.22 * .02	3.10 * .13	2.18-01 * .19-01
3.25	2.8+16	3.12 * .02	2.93 * .10	1.28-01 * .11-01
3.50	2.6+16	3.02 * .02	2.92 * .11	8.60-02 * .73-02
3.75	2.4+16	2.90 * .02	2.85 * .11	5.43-02 * .45-02
4.00	2.2+16	2.81 * .02	2.70 * .09	2.78-02 * .20-02
4.25	2.0+16	2.68 * .02	2.67 * .09	1.78-02 * .16-02
4.50	1.8+16	2.63 * .02	2.57 * .06	1.19-02 * .82-03

TABLE 5-1 (E)

EXPERIMENT NO. : 11 DENSITY SET : HIGH GAS : N

TIME (US)	NE (CM-3)	LTE KT (EV)	S-C KT (EV)	S/ALPHA
.25	7.6+15	2.83 * .02	2.29 * .12	2.66-01 * .68-01
.50	1.4+16	2.97 * .02	2.71 * .25	3.34-01 * .16+00
.75	2.0+16	3.16 * .02	2.31 * .10	3.38-01 * .10+00
1.00	2.8+16	3.30 * .02	2.40 * .10	4.58-01 * .10+00
1.25	4.6+16	3.41 * .02	2.62 * .12	4.12-01 * .12+00
1.50	6.5+16	3.51 * .02	2.67 * .10	1.95-01 * .30-01
1.75	8.6+16	3.60 * .02	2.38 * .08	6.90-02 * .12-01
2.00	1.0+17	3.71 * .03	2.44 * .06	5.59-02 * .43-02
2.25	1.1+17	3.81 * .03	2.54 * .06	9.35-02 * .79-02
2.50	1.2+17	3.76 * .03	2.87 * .08	2.01-01 * .16-01
2.75	1.1+17	3.54 * .02	2.87 * .07	1.86-01 * .15-01
3.00	9.4+16	3.35 * .02	2.69 * .06	1.30-01 * .99-02
3.25	7.4+16	3.22 * .01	2.69 * .05	1.07-01 * .70-02
3.50	6.2+16	3.10 * .01	2.70 * .04	8.24-02 * .37-02
3.75	5.2+16	3.02 * .01	2.70 * .04	7.58-02 * .33-02
4.00	4.4+16	2.93 * .01	2.61 * .03	6.43-02 * .27-02
4.25	3.8+16	2.84 * .01	2.52 * .02	5.11-02 * .17-02
4.50	3.0+16	2.76 * .01	2.45 * .02	3.80-02 * .87-03

TABLE 5-1 (F)

EXPERIMENT NO. : 16 DENSITY SET : HIGH GAS : N+HE

TIME (US)	NE (CM-3)	LTE KT (EV)	S-C KT (EV)	S/ALPHA
.25	7.6+15	2.58 * .02	1.40 * .03	3.63-02 * .10-01
.50	1.4+16	2.71 * .02	1.73 * .08	4.35-02 * .97-02
.75	2.0+16	2.86 * .02	1.45 * .03	6.70-02 * .16-01
1.00	2.8+16	3.10 * .03	1.27 * .02	1.44-01 * .38-01
1.25	4.6+16	3.39 * .04	1.29 * .02	3.42-01 * .88-01
1.50	6.5+16	3.58 * .04	1.44 * .05	6.09-01 * .15+00
1.75	8.6+16	3.67 * .04	2.26 * .15	7.53-01 * .13+00
2.00	1.0+17	3.75 * .04	2.57 * .18	1.12+00 * .19+00
2.25	1.1+17	3.77 * .04	3.00 * .31	1.07+00 * .17+00
2.50	1.2+17	3.70 * .04	3.18 * .32	8.30-01 * .13+00
2.75	1.1+17	3.57 * .03	3.02 * .20	4.90-01 * .70-01
3.00	9.4+16	3.41 * .02	2.83 * .12	2.62-01 * .36-01
3.25	7.4+16	3.23 * .03	2.67 * .08	1.37-01 * .17-01
3.50	6.2+16	3.08 * .03	2.51 * .05	7.09-02 * .72-02
3.75	5.2+16	2.96 * .03	2.40 * .05	4.77-02 * .55-02
4.00	4.4+16	2.86 * .03	2.51 * .07	3.72-02 * .41-02
4.25	3.8+16	2.74 * .03	2.33 * .07	2.10-02 * .25-02
4.50	3.0+16	2.62 * .03	2.20 * .07	1.18-02 * .16-02

CHAPTER 5

RESULTS AND DISCUSSION

A large amount of data was obtained from the computer programs; the final results (electron density N_e, LTE temperature kT_e, Semi-Corona (S-C) temperature kT_e and S/α) for each of the six experiments (three density sets each using pure N and N + He) are given in Table 5-1 (a-f).

5.1 Temperatures

The values of kT_e obtained from the LTE and Semi-Corona programs for the three sets of experiments are plotted with respect to time in Fig. 5-1 (a-c). The error bars shown represent the statistical standard deviation of the mean in each case as calculated in the programs. The LTE temperature is the mean of 63 values while the Semi-Corona kT_e is the mean of 21, which partly accounts for the smaller standard deviations in the LTE temperatures. The values of kT_e during the heating and compression phase (up to 2.25 μsec) are not expected to be very meaningful because of the non-equilibrium state of the plasma; this is evidenced by the erratic behaviour of the Semi-Corona kT_e during this time.

It can be seen that the Semi-Corona and LTE models give essentially the same temperatures in the medium density region (Fig. 5-1(b)), whereas for both the high and low density regions the temperatures obtained from the two models are quite different (Fig. 5-1 (a) and (c)). In the medium density region the two models are therefore either equally good or equally bad, and one can then take this as the approximate N_e "boundary" between the domains of validity of the two models. This gives an estimate in the region of 3×10^{16} cm^{-3} for the N_e lower limit for the validity of the LTE relation at a temperature of about 3 eV. This may be compared with the various theoretical estimates shown in Fig. 3-1; this estimate will be better justified and the matter further discussed in section 5.3.

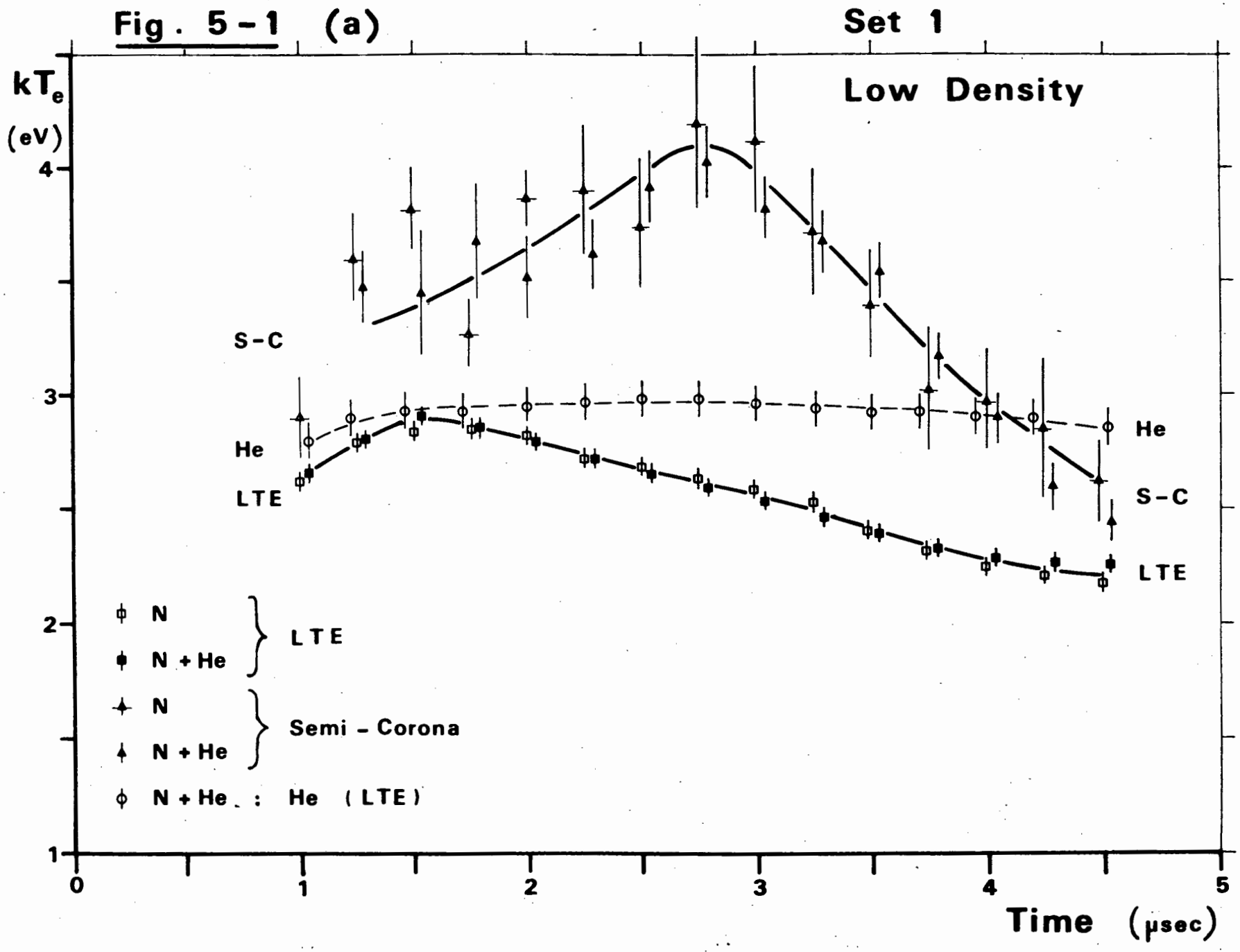
Fig. 5-1 (a)
Set 1
Low Density
kTe
(eV)
4
3
2
1
0
1
2
3
4
5
Time (μsec)
S-C
He
LTE
He
S-C
LTE
N
N + He
LTE
N
N + He
Semi - Corona
N + He : He (LTE)

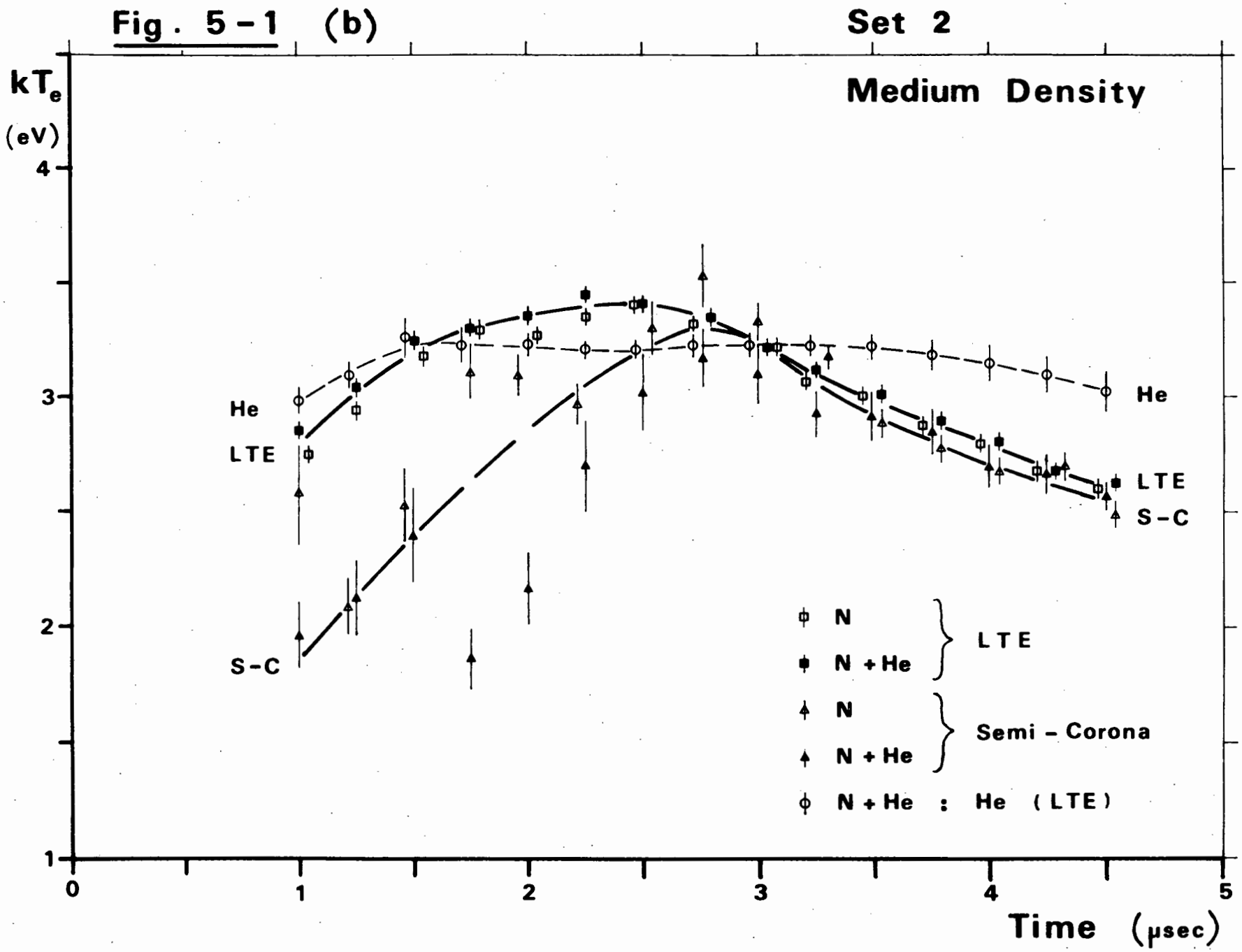
Fig. 5-1 (b)
Set 2
Medium Density
kTe
(eV)
4
3
2
1
0
1
2
3
4
5
Time (μsec)
He
LTE
S-C
He
LTE
S-C
N
N + He
LTE
N
N + He
Semi - Corona
N + He : He (LTE)

Fig. 5-1 (c)

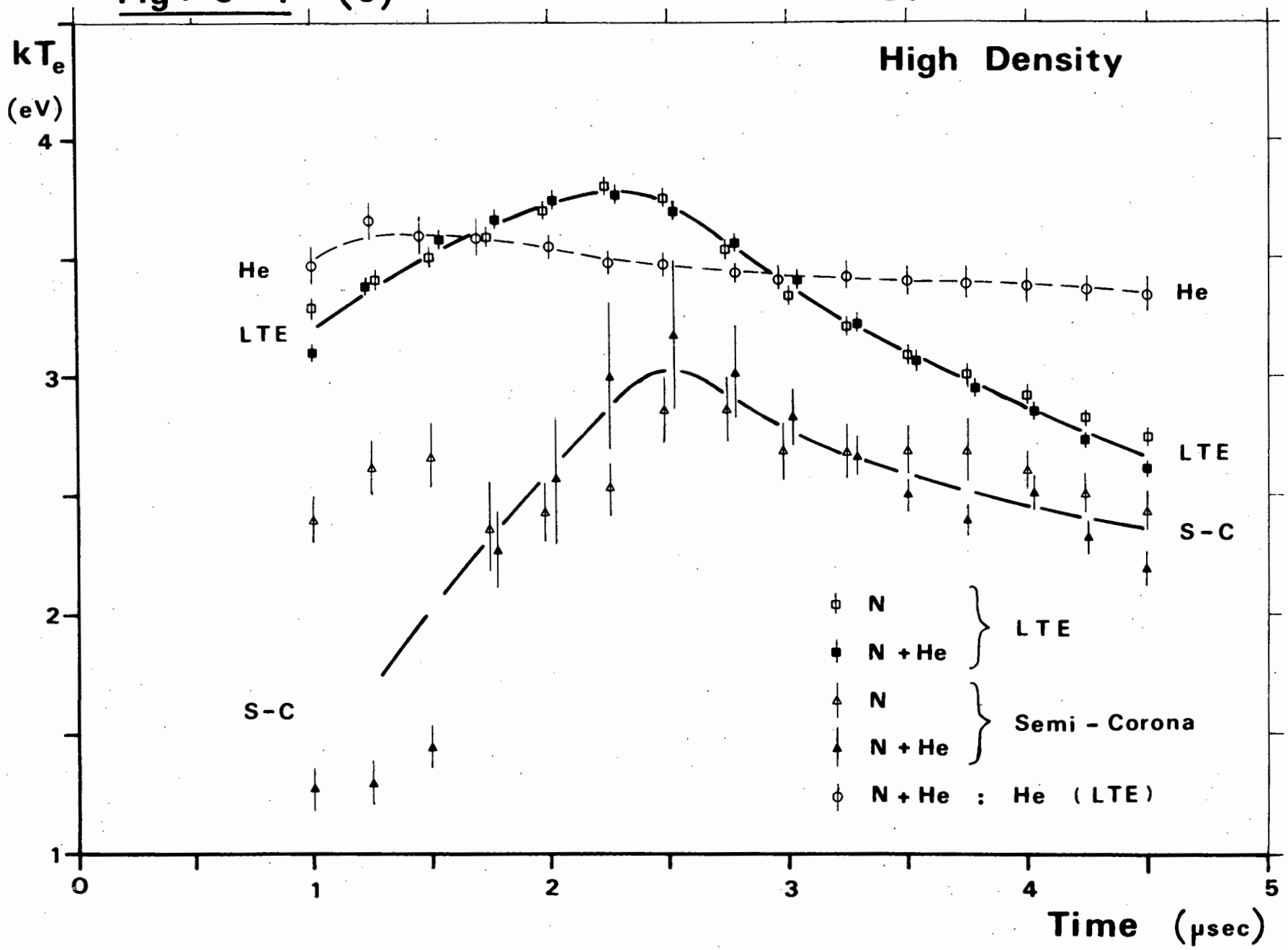
Set 3
High Density
kT_e
(eV)
4
3
2
1
0
1
2
3
4
5
Time (μsec)
He
LTE
He
LTE
S-C
S-C
N
N + He
LTE
N
N + He
Semi - Corona
N + He : He (LTE)

To check which temperatures are correct in each set, we require to measure kT_e by another method. Unfortunately, no truly independent method was available to us. However an attempt was made to determine kT_e in the N+He plasmas from measured HeII/HeI line intensity rations. Griem (1964) has plotted the intensity ratio HeII 4686 Å/HeI 5876 Å against kT_e for $N_e < 10^{18}$ cm^{-3} using an "average" of the LTE and Semi-Corona relations; however it was considered preferable to use a number of line ratios, viz. the six from the two HeII and three HeI lines given in Table 4-2, and determine kT_e using the LTE relation. Thus it was hoped that at least the consistency of the method could be checked. The results from the He measurements are also plotted in Fig. 5-1 (a-c). It can be seen that these temperatures agree reasonably well with the nitrogen LTE values in the region of the temperature peak (i.e. at about 2.5 usec); however the helium kT_e's decrease much more slowly with time than the nitrogen values in all cases.

The LTE formula is not expected to be the correct one to use for the low density set (from our earlier considerations and since we are here below the lowest predicted N_e limit for LTE), so that the nitrogen and helium LTE calculations could give "different wrong values" in this case.

However, the discrepancy between the N and He LTE temperatures in the medium and high density regions needs to be considered more thoroughly. Although the various atomic constants should be more accurate for He than for N, the probable errors in the nitrogen kT_e values are much reduced, thanks to the larger number of lines used. Also, the time variation of the nitrogen LTE temperature for the two higher density cases seems more sensible than that of the He value, since the actual temperature is expected to fall off rapidly after the peak of the theta-pinch coil current. Thus the nitrogen values are probably the more reliable of the two LTE temperatures. This may be further justified by the following argument. If in the N + He mixture each gas separately obeys its own validity criteria for LTE, and if the appropriate LTE N_e limit for nitrogen is lower than that for helium (as

is expected theoretically), then the former may be in LTE while the latter is still in the Semi-Corona domain. Thus the He LTE temperature could still be wrong even in the high density region. Unfortunately it was not possible to use the Semi-Corona method for He as the number of available lines was too small for the type of data treatment applied to the nitrogen measurements. The use of Griem's (1964) graph, mentioned above, gave considerably higher temperatures than any of the other values (typically 5 eV) and these also remained practically constant in time. This would appear to be anomalous; however, the "averaging" procedure over the Semi-Corona and LTE methods used to obtain the graph is not clear.

The work of Eckerle and McWhirter (1966) should be mentioned here. They measured the temperature in an H + He plasma at $N_e \sim 10^{15}$ cm^{-3} using the Balmer discontinuity method, and simultaneously measured the HeII 4686/ HeI 5876 intensity ratio. The temperature determined from the latter using the LTE formula decreased very slowly in time, while that from the former peaked at a much higher value and fell off much more rapidly. It was concluded from other considerations that their plasma was not in LTE, so that this (a constant low value) would appear to be the behaviour of the He LTE temperature at densities below the LTE limit. Eckerle and McWhirter (1966) suggest that a possible cause of this behaviour is the trapping of HeII resonance radiation (λ= 304 Å for the first resonance line) emitted, in the case of their shock-heated plasma, from another part of the shock (i.e. external to the studied plasma). The HeII ions in the ground state would then be raised to the first excited level and recombination would be inhibited. However, this would not appear to be valid in our case.

For the LTE line intensity ratio formula to be applicable we require the upper ionization stage (in this case HeII) to be in complete LTE (see section 4.3.1), so the appropriate LTE limit is that for complete LTE in HeII. At kT_e = 3 eV, Griem's (1964) estimate for this limit is $N_e = 1.2 \times 10^{18}$ cm^{-3} (see section 3.2, eq. (3.5)), and we expect this estimate for the hydrogenic ion HeII to be more reliable than those for the N ions.

Thus the He LTE temperature does not appear to be valid, even in our high density region, and we must, unfortunately, conclude that an independent check of the nitrogen kT_e values was not possible.

It appears from our results that the use of the 50% N + He mixture in place of pure nitrogen does not appreciably affect the temperature determined from the nitrogen line intensities using either of the two models and for all three density regions (see Fig. 5-1 (a-c)).

Finally, it must also be mentioned that the helium LTE temperatures in the N + He plasmas were, for each density set, within 10% of those measured in the H + He plasmas, where N_e was also determined (section 4.2.2). This can be taken as indicating support for the assumption made in that section that N_e was the same in these two plasmas for the same initial conditions, as, even though the He LTE temperatures are wrong, they should still be the same ("equally wrong") at the same density.

5.2 S/α Values

In the Semi-Corona program, the minimum percentage standard deviation amongst the S/α values for each combination of two NIII lines (at the "true" kT_e parameter value) was typically 30-40%, although considerably higher (> 60%) minimum deviations occurred in some cases. The minimum position was well defined, as, for a typical minimum deviation of 30%, the deviation increased to 80-100% at about 1 eV on either side of the minimum position. The average values of S/α from the different combinations generally differed by less than an order of magnitude. In one or two cases where this was not true the NIII line concerned was omitted from the analysis.

The S/α values obtained at times later than that of the temperature peak (i.e. from 2.5 or 2.75 usec to 4.5 usec) are plotted against the Semi-Corona (S-C) kT_e for the three sets of experiments in Fig. 5-2 (a-c) where the logarithmic dependence of S/α on kT_e is shown. Also plotted on the same graph for each set is the Saha ratio of NIV : NIII ground state populations

Fig. 5-2 (a)

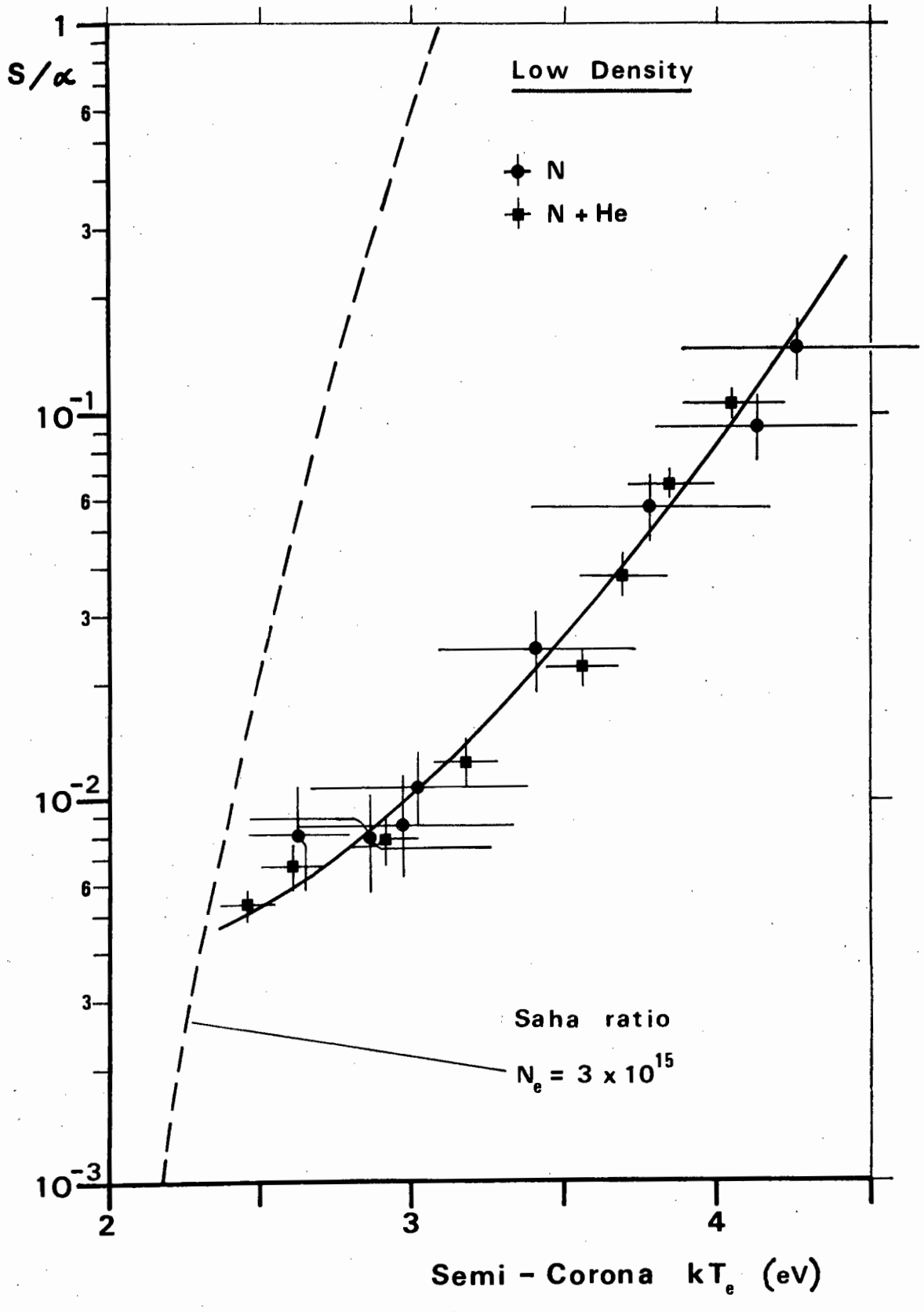
S/α
1
6
3
10^-1
6
3
10^-2
6
3
10^-3
Low Density
N
N + He
Saha ratio
N_e = 3 x 10^15
2
3
4
Semi - Corona kT_e (eV)

Fig. 5-2 (b)

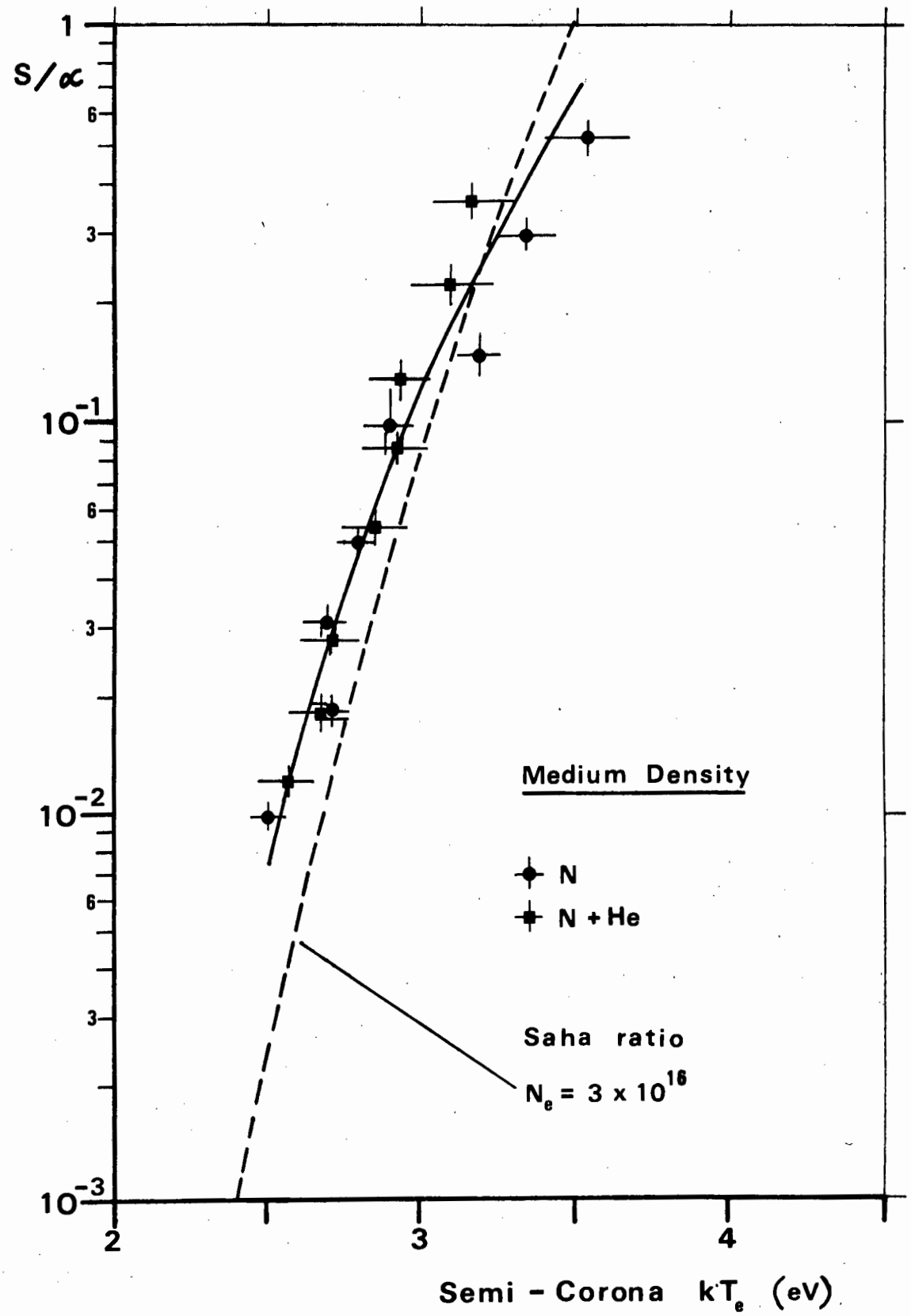
S/α
1
6
3
10^-1
6
3
10^-2
6
3
10^-3
2
3
4
Semi - Corona kT_e (eV)
Medium Density
N
N + He
Saha ratio
N_e = 3 x 10^16

Fig. 5-2 (c)

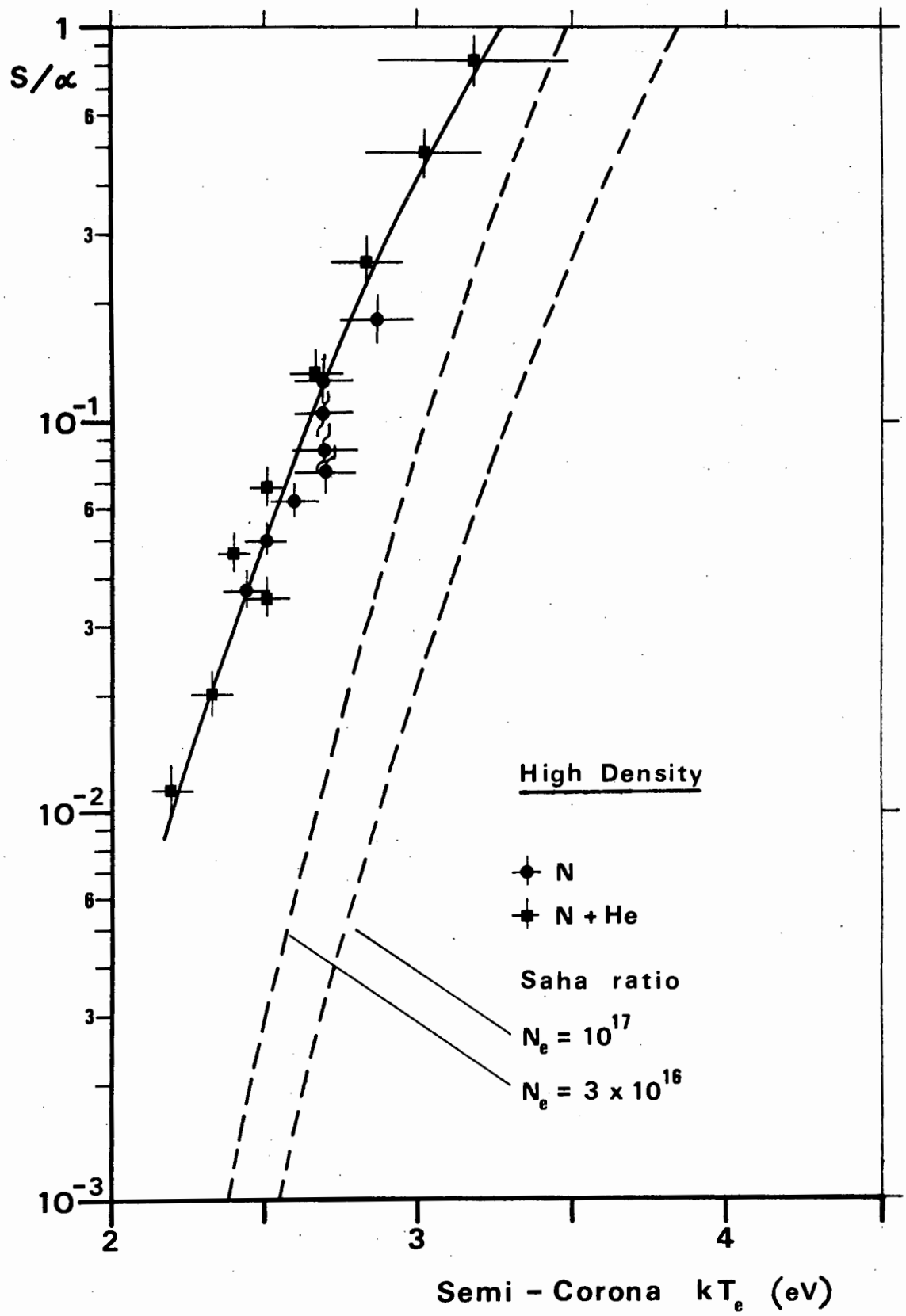
S/α
1
6
3
10^-1
6
3
10^-2
6
3
10^-3
2
3
4
Semi - Corona kT_e (eV)
High Density
N
N + He
Saha ratio
N_e = 10^17
N_e = 3 x 10^16

Fig. 5-2 (d)

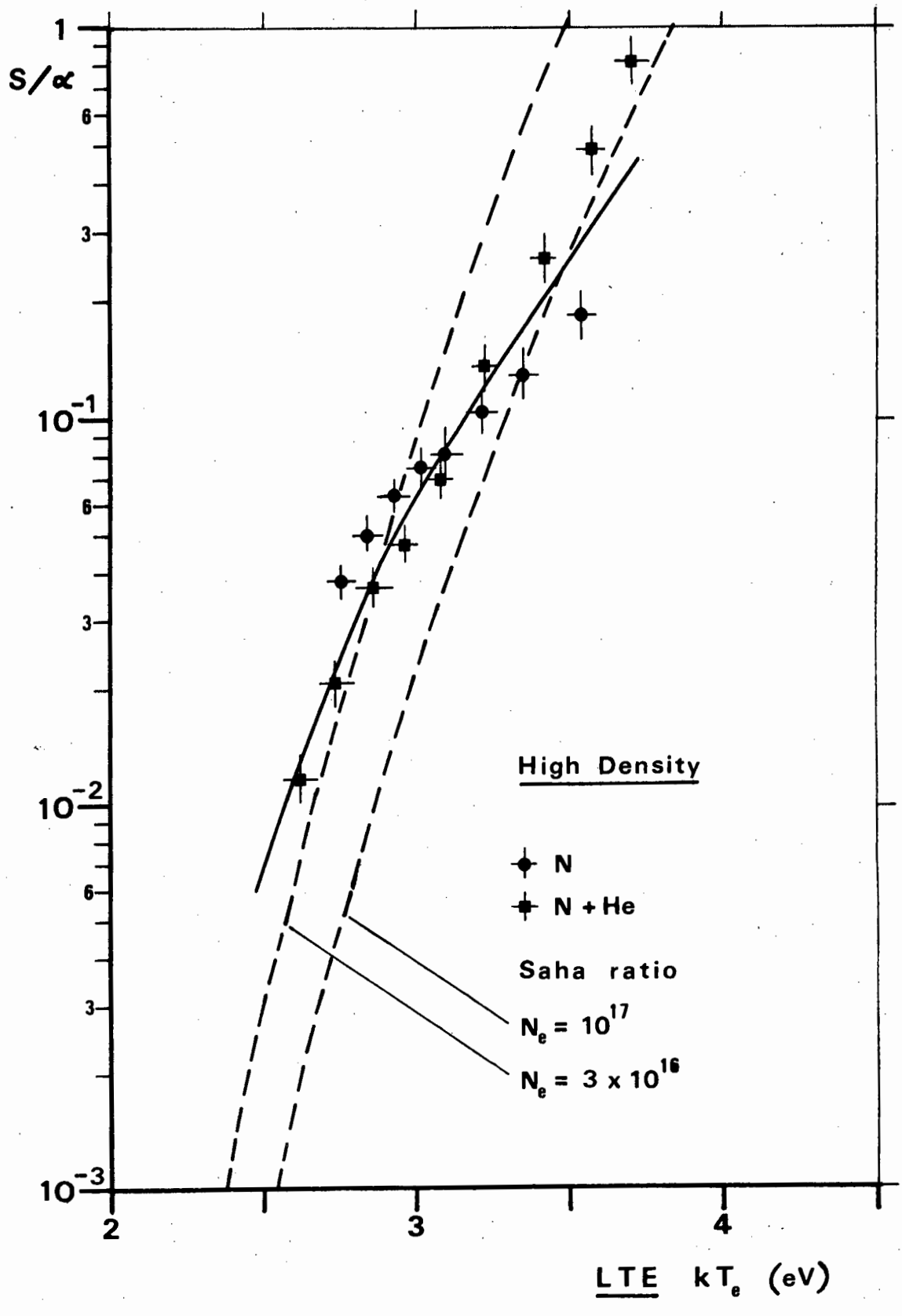
S/α
1
6
3
10^-1
6
3
10^-2
6
3
10^-3
2
3
4
LTE kT_e (eV)
High Density
N
N + He
Saha ratio
N_e = 10^17
N_e = 3 x 10^16

at approximately the appropriate electron density. It can be seen that for the low density set (Fig. 5-2(a)) the S/α values lie below the Saha ratio at a particular temperature; for the medium density set (Fig. 5-2(b)) the two ratios are approximately equal, and in the high density case (Fig. 5-2(c)) the S/α values are noticeably higher than the Saha ratio.

Now the Saha ratio is the upper limit of the actual ionization ratio (Bates et al. (1962)), i.e. of the ratio S/α; this limit is reached at the "boundary" between the Semi-Corona and LTE domains. In terms of the intensity ratios, this is illustrated by equating the two expressions for I'/I, viz. equations (4.8) and (4.11); we have at the boundary

$$\frac{S'}{\alpha''}\frac{g_1'}{g_1''}\quad\frac{f'g'\lambda^3}{fg\lambda'^3}\quad\exp\left(\frac{E_\infty'-E'-E_\infty+E}{kT_e}\right)=\frac{2}{N_e}\quad\frac{f'g'\lambda^3}{fg\lambda'^3}\left(\frac{m_ekT_e}{2\pi\hbar^2}\right)^{3/2}$$

$$\exp-\left(\frac{E'+E_\infty-E}{kT_e}\right) \qquad (5.1)$$

so that

$$\frac{S'}{\alpha''}=\frac{2}{N_e}\quad\frac{g_1''}{g_1'}\left(\frac{m_ekT_e}{2\pi\hbar^2}\right)^{3/2}\cdot\exp\frac{E'}{kT_e}=\frac{N_1''}{N_1'}\ \text{(Saha)} \qquad (5.2)$$

the Saha ratio of ground state populations, ionization stages prime and double prime.

It is clear, therefore, that from consideration of the relative values of S/α and the Saha ratio in a particular density region, conclusions may be drawn about the validity of the two plasma models in that region. The fact that our measured values of S/α for the high density set are apparently higher than the Saha ratio would seem to indicate that the Semi-Corona model is no longer applicable and that this set lies in the LTE regime. If this is true then the Semi-Corona temperature is wrong and it would be more appropriate to plot these S/α values against the LTE temperature. (It is necessary to assume

Fig. 5-3

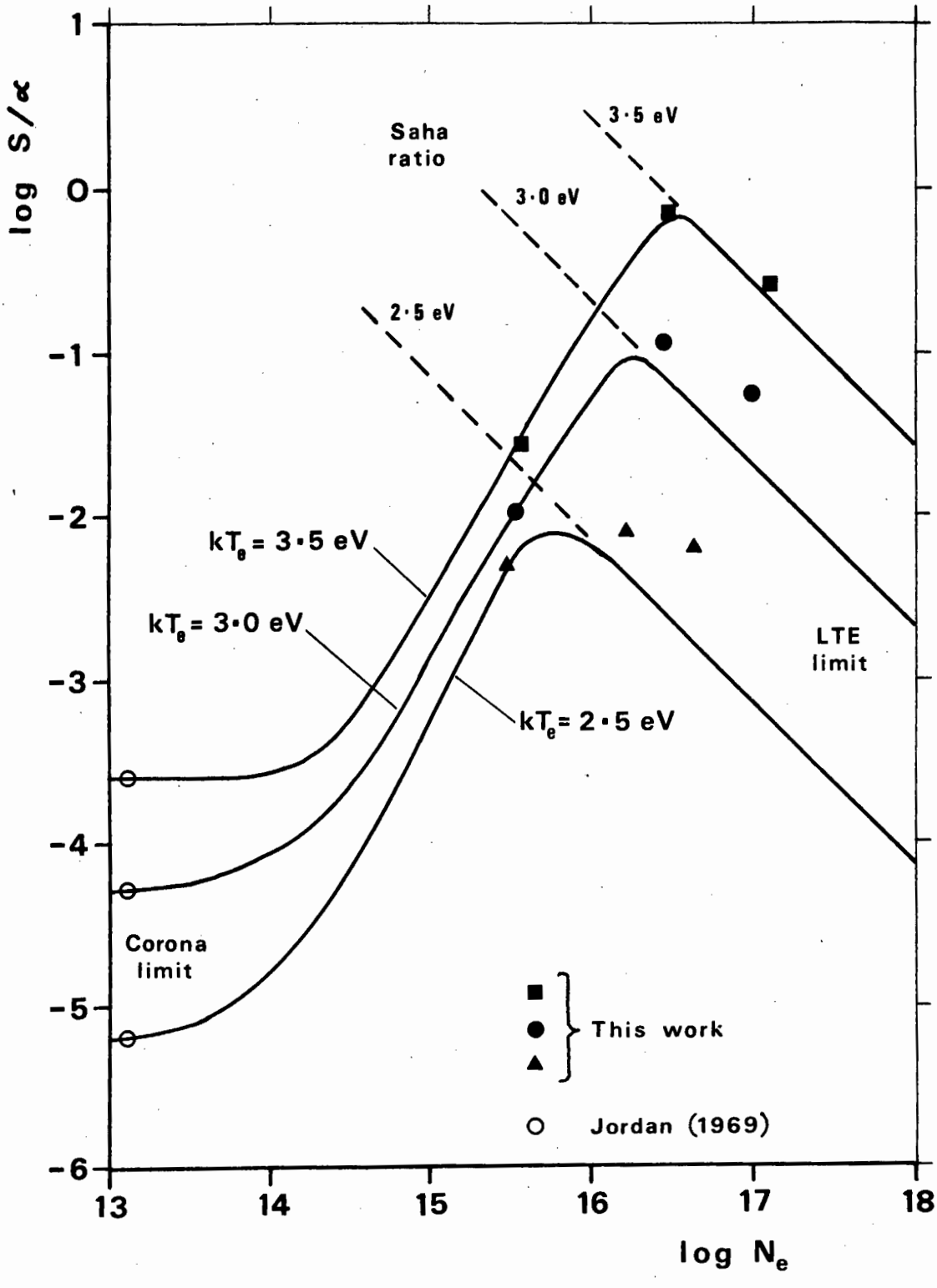
log S/κ
1
0
-1
-2
-3
-4
-5
-6
13
14
15
16
17
18
log N_e
Saha ratio
3·5 eV
3·0 eV
2·5 eV
kT_e = 3·5 eV
kT_e = 3·0 eV
kT_e = 2·5 eV
LTE limit
Corona limit
This work
Jordan (1969)

here that S/α and the Semi-Corona kT_e are independent variables; this is valid, as, for instance, doubling all the S/α values for the different line pairs would not affect the value of the parameter kT_e at which the deviation amongst these S/α values was a minimum, i.e. the "true" kT_e, while the average S/α would be doubled). The S/α values for the high density set are plotted against the LTE kT_e in Fig. 5-2(d) where it is seen that, in the N + He case at least, agreement with the Saha ratio is fairly close. (The actual Saha ratio will move between the "$N_e = 10^{17}$" curve - the electron density at the earliest time (2.75 μsec) - and the "$N_e = 3 \times 10^{16}$" curve - the electron density at the latest time (4.5 μsec)). Thus we have S/α, and therefore the ionization ratio, following the Saha ratio once the LTE domain is reached, as expected. (It was seen that the two ratios were approximately equal at the medium density).

The S/α values for the low density set show that this set lies in the Semi-Corona regime as they lie between the "low density" (i.e. Corona model limit) values of Jordan (1969) and the Saha ratio at the same density and temperature, as indicated in Table 5-2 below.

Table 5-2: S/α values

kT_e (eV)	Jordan[1]	This Work[2]	Saha ratio[3]
2.5	7.0×10^{-6}	5.4×10^{-3}	2.4×10^{-2}
3.0	5.0×10^{-5}	1.1×10^{-2}	6.2×10^{-1}
3.5	2.5×10^{-4}	2.7×10^{-2}	7.0×10^{0}

(1) Interpolated or slightly extrapolated from given values

(2) Taken from the "best fit" curve, Fig. 5-2(a)

(3) $N_1(\text{NIV})/N_1(\text{NIII})$ at $N_e = 3 \times 10^{15}$ cm^{-3}

The S/α values from each of the three density sets at each of the three temperatures 2.5, 3.0 and 3.5 eV, taken from the "best fit" curves, Fig. 5-2 (a), (b) and (d) respectively are plotted against N_e in Fig. 5-3, where Jordan's

(1969) values and the Saha ratios are also indicated. The curves show the expected form of variation of the ionization ratio with respect to electron density, and may be compared with those for hydrogen given in Fig. 2-1 (c).

It is not clear how our results compare with the calculations of Kulander (1965), as in his paper (mentioned in section 2.3) he only gives the "nitrogen non-equilibrium populations" at temperatures of 10^4, 10^5 and 10^6 ^oK (0.86, 8.6 and 86 eV). The values of the NIV : NIII ground state population ratio N_1^4/N_1^3 at $N_e = 10^{15}$ cm^{-3} obtained from his calculations are approximately 10^{-18} at $T_e = 10^4$ ^oK (kT_e = 0.86 eV) and 10^5 at $T_e = 10^5$ ^oK (kT_e = 8.6 eV) for "dilution factor" W = 1; and 40 at $T_e = 10^5$ ^oK for W = 0 (values at $T_e = 10^4$ ^oK for W = 0 are not given). Interpolation between these values is not possible.

5.3 N_e Limit for Complete LTE in NIII

In Chapter 2 (equation (2.2)), we defined the parameter

$$b_p = \frac{N_p^z\ (CR)}{N_p^z\ (Saha)} \qquad (5.3)$$

where N_p^z(CR) and N_p^z(Saha) are the (relative) populations of state p, ionization stage z is determined from the collisional-radiative model and Saha equations respectively. (We have $b_p \leq 1$, with equality holding in LTE). Measurements of this parameter were used by Berg (1967) to determine possible deviations from LTE in OII, with p the 4f level, its population being determined relative to the 3p level. (In fact no deviations from $b_p = 1$ were detected down to the lowest N_e value in the experiment, viz. 10^{16} cm^{-3}).

If, for our purposes, p is taken to be the NIV ground state (i.e. p = 1, z = 4), with its population measured relative to the NIII ground state, we then have

$$b_1 = \frac{S'/\alpha''}{N_1''/N_1'\ (Saha)} \qquad (5.4)$$

where prime and double prime denote NIII and NIV respectively.

The values of b_1 at each of the three temperatures (2.5, 3.0 and 3.5 eV) for the three density sets, with S/α taken from the appropriate graph (Fig. 5-2(a), (b) or (d)) and the Saha ratio calculated for that kT_e and the N_e at the time at which that S/α and kT_e were attained, are plotted against N_e in Fig 5-4(a). Since the "real" b_1 cannot be greater than unity it would appear reasonable to take the N_e value at which our experimental $b_1 = 1$ to be the lower limit of validity for the LTE line intensity ratio relation (4.8). This relation assumes NIII to be in complete LTE and the upper levels of the NII lines used to be above the thermal limit (see section 4.3.1). Since the second condition is already assumed in applying the Semi-Corona relation (section 4.3.2), it is thus apparent that N_e ($b_1 = 1$) represents the lower limit for complete LTE in NIII at each of three temperatures. The values obtained from Fig. 5-4(a) are:

kT_e (eV)	$N_e(b_1 = 1)$ (cm^{-3})
2.5	1.2×10^{16}
3.0	2.4×10^{16}
3.5	3.5×10^{16}

The temperature dependence of the N_e LTE limit inferred from these results is stronger than the square-root dependence predicred by all the authors considered (except Drawin (1969) who predicts a weaker dependence); this can be seen in Fig. 3-1 where the above three N_e - kT_e points are plotted (the points x) for the purpose of comparison with the various theoretical estimates. However, it is not felt that much confidence can be placed in any inferred temperature dependence because of the small range of kT_e covered and because the uncertainty in each of these values could easily be 20% or more.

Fig. 5-4

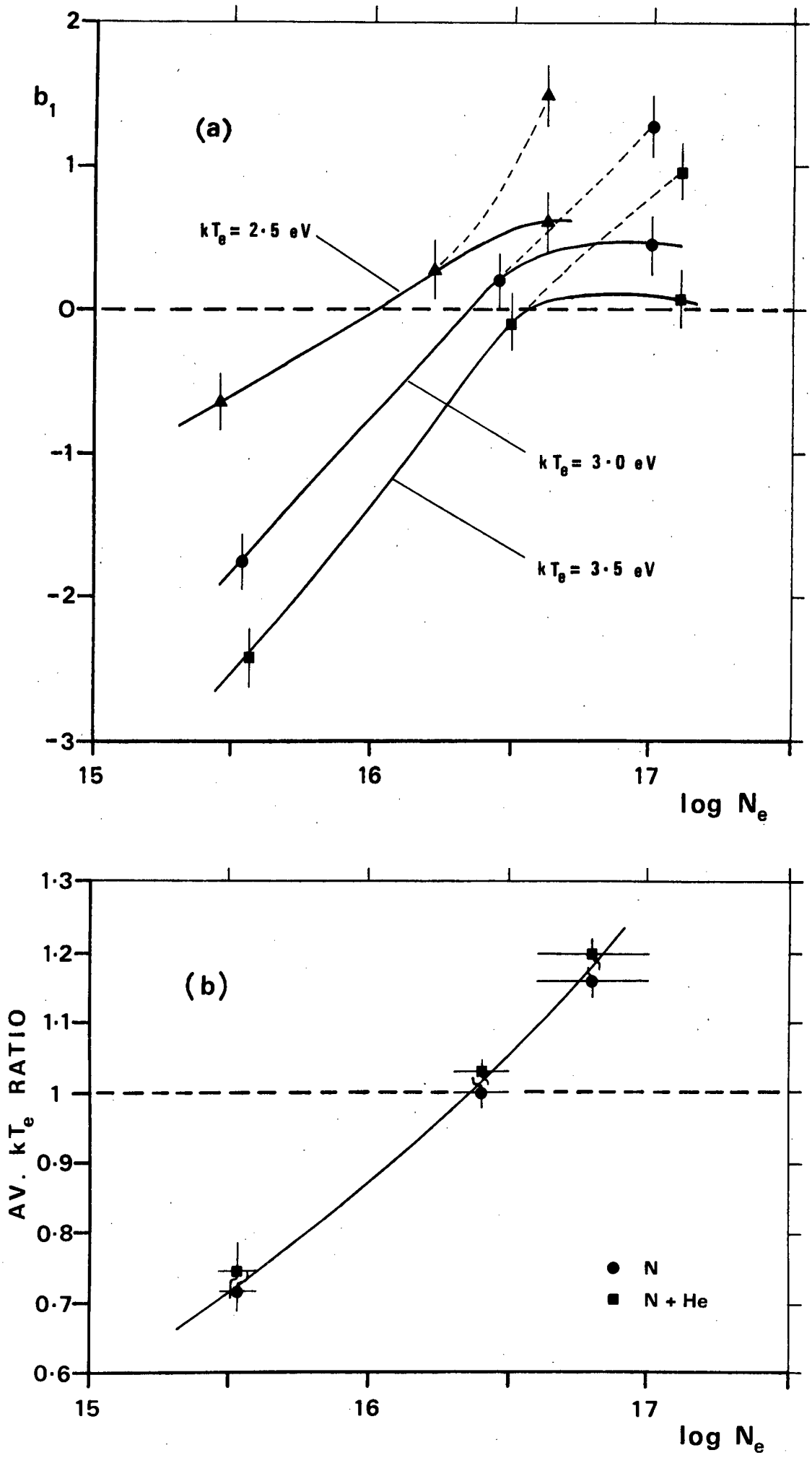
(a)
b_1
2
1
0
-1
-2
-3
kT_e = 2·5 eV
kT_e = 3·0 eV
kT_e = 3·5 eV
15
16
17
log N_e
(b)
AV. kT_e RATIO
1·3
1·2
1·1
1
0·9
0·8
0·7
0·6
N
N + He
15
16
17
log N_e

Greater confidence can probably be attached to the average value of 2.3 x 10^{16} cm^{-3} as an estimate of the N_e lower limit for complete LTE in NIII for kT_e approximately 3 eV.

It can be seen from Fig. 3-1 and Table 3-2 (where the various theoretical estimates at kT_e = 3eV are given) that this average value (the middle x in Fig. 3-1) is a factor ~3 higher than the estimates made from Griem (1964) and Drawin (1969) but a factor ~50 or more lower than the estimates of Kulander (1965) and Wilson (1962). It therefore appears that the use of the maximum energy gap (for the first two estimates) is more realistic than the use of the ionization energy (for Wilson's estimate) or an assumed simplified level system (for Kulander's).

Finally, we return to the question of the correctness of the two temperatures (Semi-Corona and LTE) in each density region raised in section 5-1. The ratio LTE kT_e/S-C kT_e was determined for each of the six experiments at each time from the temperature peak on (i.e. 2.75 to 4.5 usec) and an average of this ratio, as well as an average N_e, over these times, determined for each experiment. The resulting plot of average temperature ratio against electron density is shown in Fig. 5-4(b). The fitted curve attains the value 1 (i.e. LTE kT_e - Semi-Corona kT_e) at N_e = 2.2 x 10^{16} cm^{-3}, which practically coincides with the average value of N_e (b_1 = 1). Thus it appears that the LTE : Semi-Corona temperature ratio could be used as an alternative indicator of the attainment of LTE and that whichever of the two temperatures is higher indicates the correct model to use (i.e. the higher of the two temperatures is always correct).

5.4 Errors

The main sources of error in the measurement of the intensity ratios arise from the plasma itself. Since each line intensity was measured in a different shot, we assume that the same plasma is produced, and that we observe the same point in the plasma (with the same actual temperature and density), in each case. Reproducibility was checked in each run by repeating the measurements

on a few lines at random, and was found to be generally within about 10%. Where serious non-reproducibility did occur, it was usually found to be due to fluctuation in the firing time of the crowbar switches (and hence in the energy supplied to the theta-pinch coil). Checking the reproducibility of the coil current from shot to shot was one reason for monitoring this current simultaneously with the line intensity, as mentioned in section 4.1.2. The three crowbar switches in parallel replaced the single switch employed in the experiments described in Cilliers, Hey and Rash (1973) and Hey (1970). This resulted in a much smoother (closer to a smooth exponential) coil current. In addition the coil current was actually crowbarred slightly after the current peak; this reduced "jitter" and improved the reproducibility but also considerably reduced the duration of the coil current. Also in the present work the time constant of the photomultiplier output circuit was reduced from a considerably higher earlier value to about 0.2 μsec. The gun, in its final form, was found to be reproducible to within the same margin as the main bank, i.e. about 10%.

Another source of error enters the calculations in that the oscillator strengths of the lines are not very accurately known and could give rise to appreciable errors in S/α, etc. The f values obtained from Wiese, Smith and Glennon (1966) are all estimated to have an uncertainty of under 25% (accuracy "C" in their notation), and the same uncertainty should apply to the three values taken from Griem (1964) (see Table 4-2). Probably the most uncertain f value is that of the NIII line 4379 Å; the value used was taken from Allen (1955). This is a 4f - 5g transition, so f cannot be calculated using the Bates and Damgaard (1949) tables, as these are only for s-p, p-d and d-f transitions. Allen gives gf = 6.3 and transition probability $A = 2.2 \times 10^8$ sec^{-1}, from which f = 0.788. It is not clear what accuracy can be attached to this value. However our calculated parameter values (S/α and kT_e) involving this line did not appear to deviate consistently from those involving the other lines.

5.5 The Thermal Limit

In considering possible errors we must also examine the assumption made

in applying both the LTE and Semi-Corona relations for I'/I that the upper levels of the transitions are above the respective thermal limits n_t. The values of n_t calculated from Wilson's (1962) expression (equation (3.3)) and Griem's (1964) relation (equation (3.4)) for NII and NIII at a typical density in each of our three domains are given in Table 5-3(a) and (b) respectively. The effective charge

$$z_{eff} = \sqrt{\frac{E_\infty^z}{E_H}}$$

has been used for z in these hydrogenic expressions. For the purposes of direct comparison the quantum numbers n* of the lines used in our measurements are also given for each ion. It can be seen from Table 5-3(a) that for NII in the low density case ($N_e = 3.5 \times 10^{15}$ cm^{-3}), n* for the lines 4601, 4613 and 4630 lie slightly below n_t, but otherwise the condition $n^* > n_t$ is everywhere satisfied. For NIII (Table 5-3(b)) we see that the condition is violated for the lines 4097 and 4103 (and slightly for 4634) at the low density. Thus in the low density set we should regard as possibly unreliable the NIII lines 4097 and 4103, and to a lesser extent the three NII lines and NIII 4634. The proximity of n* to n_t for these lines at this density may account for the fact that the errors in the Semi-Corona parameters are still large, even though we expect this model to be applicable here (see Figs. 5-1(a) and 5-2(a)) (The large error bars in the pure N low density results may also be partly attributable to the fact that only five NIII lines were used instead of the seven used for all the other experiments). However, no exceptionally large deviations for the above-mentioned lines manifested themselves.

TABLE 5-3 (A) : N II

THERMAL LIMIT NT

KT (EV)	3.5+15	3.0+16	1.0+17	NE (CM-3)
2.5	2.55	1.88	1.58	
3.0	2.58	1.90	1.60	WILSON
3.5	2.61	1.92	1.62	
2.5	2.61	2.23	2.06	
3.0	2.58	2.19	2.02	GRIEM
3.5	2.56	2.16	1.98	

EFFECTIVE PRINCIPAL QUANTUM NUMBER OF UPPER LEVEL N*

LINE	N*
3919	3.00
4145	7.02
4176	3.98
4227	3.28
4447	2.91
4601	2.54
4613	2.54
4630	2.54
4803	2.93

TABLE 5-3 (B) : N III

THERMAL LIMIT NT

KT (EV)	3.5+15	3.0+16	1.0+17	NE (CM-3)
2.5	3.12	2.30	1.93	
3.0	3.16	2.33	1.96	WILSON
3.5	3.20	2.35	1.98	
2.5	3.07	2.62	2.43	
3.0	3.04	2.57	2.37	GRIEM
3.5	3.02	2.54	2.33	

EFFECTIVE PRINCIPAL QUANTUM NUMBER OF UPPER LEVEL N*

LINE	N*
3754	3.80
4097	2.68
4103	2.68
4379	4.98
4514	3.68
4518	3.68
4634	2.92

ACKNOWLEDGEMENTS

I wish to express my thanks to Dr. W.A. Cilliers for supervising this project, for helpful discussions and for his advice and encouragement.

My thanks also go to Mr. D. Momsen for his work in developing some of the apparatus and technical assistance, and to Mrs. P. Dobbie for her painstaking work of typing the manuscript.

Finally I thank the University of Cape Town for financial assistance.

BIBLIOGRAPHY

ALLEN, C.W. (1955): "Astrophysical Quantities", Athlone Press.

BATES, D.R. & A. DAMGAARD (1949): Proc. Roy. Soc. A242, 101.

BATES, D.R., A.E. KINGSTON & R.W.P. McWHIRTER (1962): Proc. Roy. Soc. A267, 297.

BERG, H.F. (1967): Z. Phys. 207, 404.

BURGESS, A. (1964): Astrophys. J. 139, 776.

BURGESS, A. (1965): Astrophys. J. 141, 1588.

BYRON, S., R.C. STABLER & P. I. BORTZ (1962): Phys. Rev. Letters 8, 376.

CILLIERS, W.A., J.D. HEY & J.P.S. RASH (1973): J. Plasma Phys. 9, 77.

COOPER, J. (1966): Rep. Prog. Phys. 29, 35.

COX, D.P. & W. H. TUCKER (1969): Astrophys. J. 157, 1157.

DRAWIN, H.W. (1969): Z. Phys. 228, 99.

ECKERLE, K.L. & R.W.P. McWHIRTER (1966): Phys. Fluids 9, 81.

FUJIMOTO, T. (1973): J. Phys. Soc. Japan 34, 216.

GREEN, L.C., P.P. RUSH & C.D. CHANDLER (1957): Astrophys. J. Suppl. Ser. 3, 37.

GRIEM, H.R. (1962): Phys. Rev. 128, 997.

GRIEM, H.R. (1963): Phys. Rev. 131, 1170.

GRIEM, H.R. (1964): "Plasma Spectroscopy", McGraw-Hill.

HEY, J.D. (1970): M.Sc. Thesis, U.C.T.

HILL, M. & R. G. MONTAGUE (1966): Culham Lab. Memo. CLM-M62 (Unpublished).

HOUSE, L.L. (1964): Astrophys. J. Suppl. Ser. 8, 307.

JORDAN, C. (1969): M.N.R.A.S. 142, 501.

KULANDER, J.L. (1965): J.Q.S.R.T. 5, 253.

McWHIRTER, R.W.P. & A.G. HEARN (1963): Proc. Phys. Soc. 82, 641.

McWHIRTER, R.W.P. (1965): Ch. 5 of "Plasma Diagnostic Techniques" (ed. R.H. Huddlestone & S.L. Leonard), Academic Press.

MOORE, C.E. (1949): "Atomic Energy Levels", N.B.S. Circular 467.

PARK, C. (1968): J.Q.S.R.T. 8, 1633.

SEATON, M.J. (1959): M.N.R.A.S. 119, 90.

SEATON, M.J. (1962): Ch. 11 of "Atomic and Molecular Processes" (ed. D.R. Bates), Academic Press.

SEATON, M.J. (1964): Planet. Space Sci. 12, 55.

SPITZER, L. (1956): "Physics of Fully Ionized Gases", Interscience.

TUCKER, W.H. & R. J. GOULD (1966): Astrophys. J. 144, 244.

WIESE, W.L. (1965): Ch. 6, op. cit. McWhirter, R.W.P. (1965).

WIESE, W.L., M.W. SMITH & B.M. GLENNON (1966): "Atomic Transition Probabilities", N.S.R.D.S. - N.B.S. 4.

WILSON, R. (1962): J.Q.S.R.T. 2, 477.

WOOLLEY, R. v.d.R. & C.W. ALLEN (1948): M.N.R.A.S. 108, 292.

APPENDIX

The computer programs RLTE and RCOR used in the analysis (sections 4.4.1 and 4.4.2) are given.

```
0/12-18:50-
      C
      C                                  ********************
      C                                  *   PROGRAM RCOR     *
      C                                  ********************
0101:       DIMENSION SUM(16),DIFS(16),TEMP(2,16)
0102:       DIMENSION AV(16,2,22),SDEV(16,2,22),RELE(16,2,22),WA(8),FA(8),G
           1),EA(8),WB(12),FB(12),GB(12),EB(12),A(8),B(12),S(8,12,16),
           2NA(22),NB(22),NI(22),TMIN(22),SMIN(22)
0103:       DIMENSION VA(8),VB(12),PMA(8),PMB(12),TIME(20),TAV(20),DEVT(20)
           1SAV(20),DEVS(20),FGW(8,12),RAT(8,12)
0104:       DIMENSION RATIO(8,12,20),TSOL(22,20),SSOL(22,20)
0105:       DIMENSION AVSA(16),DEVSA(16)
      C
      C        TIME INTERVAL , NO. OF TIMES
0106:       DATA TIMINC,ITEND/0.25,18/
      C        IOPT=0 : MIN. PERCENTAGE STD. DEV. ; IOPT=1 : MIN. STD. DEV.
      C        KT INCREMENT NO. AT WHICH TO START SEARCHING FOR MIN. DEV.
0107:       DATA IOPT/0/ISTRT/5/
      C        N III , N II IONIZATION ENERGIES
0110:       DATA EZA,EZB/382625.5,238751.1/
      C        N III / N II GROUND STATE STATISTICAL WEIGHTS ,
      C        CONVERSION CM-1 TO EV
0111:       DATA GZ/2.0/RNO/ .124E-03/
      C        NO. OF KT INCREMENTS ( IN EACH OF TWO BLOCKS )
0112:       DATA ITEMP/16/
      C        NO. OF N II LINES , NO. OF N III LINES ,
      C        NO. OF COMBINATIONS OF TWO N III LINES
0113:       DATA NTWO,NTHR,LCHK/9,7,22/
      C        N III LINE NOS. IN EACH COMBINATION
      C        ( E.G. COMBIN. NO. 3 IS LINES 1 & 4 )
0114:       DATA(NA(L),L=1,22)/1,1,1,1,1,1,2,2,2,2,2,3,3,3,3,4,4,4,5,5,6,1/
0115:       DATA(NB(L),L=1,22)/2,3,4,5,6,7,3,4,5,6,7,4,5,6,7,5,6,7,6,7,7,7/
0116:       DATA(NI(L),L=1,22)/1,2,3,4,5,6,1,2,3,4,5,1,2,3,4,1,2,3,1,2,1,1/
      C        PRINT OPTION ON DETAILED VALUES
0117:       DATA IPRNT/1/IPST/12/
      C        GAS : 7 = NITROGEN , 2 = HELIUM
0120:       DATA IGAS/7/
      C
      C        INPUT FIXED DATA ARRAY : WAVELENGTH , F , G , ENERGY
      C        ( J = N III LINE INDEX , K = N II LINE INDEX )
      C
0121:       DO 11 J=1,NTHR
0122:    11 READ(8,102) WA(J),FA(J),GA(J),EA(J)
0123:       DO 12 K=1,NTWO
0124:    12 READ(8,102) WB(K),FB(K),GB(K),EB(K)
0125:       DO 81 J=1,NTHR
0126:       DO 81 K=1,NTWO
0127:       FGW(J,K)=FB(K)*GB(K)*((WA(J)/WB(K))**3)/(GZ*FA(J)*GA(J))
0130:    81 CONTINUE
      C
      C        INPUT VOLTAGE SCALE FACTORS , PM RESPONSE FACTORS
0131:       READ(8,125)(VA(J),J=1,NTHR)
0132:       READ(8,125)(VB(K),K=1,NTWO)
0133:       READ(8,126)(PMA(J),J=1,NTHR)
0134:       READ(8,126)(PMB(K),K=1,NTWO)
      C
```

```
0135:       WRITE(5,117)
0136:       WRITE(5,118)(J,WA(J),FA(J),GA(J),EA(J),J=1,NTHR)
0137:       WRITE(5,119)
0140:       WRITE(5,118)(K,WB(K),FB(K),GB(K),EB(K),K=1,NTWO)
0141:       WRITE(5,120)
0142:       WRITE(5,123)
      C
      C         SET TIME ; INPUT INTENSITIES , MULTIPLY
      C         BY FACTORS & CALCULATE RATIO
      C
0143:       IT=1
0144:    13 T=IT
0145:       TIME(IT)=T*TIMINC
      C
0146:       READ(8,104)(A(J),J=1,NTHR)
0147:       READ(8,104) (B(K),K=1,NTWO)
      C
0150:       DO 51 J=1,NTHR
0151:       A(J)=A(J)*VA(J)
0152:       A(J)=A(J)*PMA(J)
0153:    51 CONTINUE
0154:       DO 52 K=1,NTWO
0155:       B(K)=B(K)*VB(K)
0156:       B(K)=B(K)*PMB(K)
0157:    52 CONTINUE
0160:       DO 82 J=1,NTHR
0161:       DO 82 K=1,NTWO
0162:       RAT(J,K)=A(J)/B(K)
0163:       RATIO(J,K,IT)=RAT(J,K)
0164:    82 CONTINUE
0165:       IF(IPRNT.EQ.0) GO TO 70
0166:       IF(IT.LE.IPST) GO TO 70
0167:       WRITE(5,105) TIME(IT)
0170:    70 CONTINUE
      C
      C         TEMP. VALUES IN TWO BLOCKS
      C
0171:       DO 14 M=1,2
0172:       DO 14 I=1,ITEMP
0173:       RI=I
0174:       RITEM=ITEMP
0175:       IF(M.EQ.1) TEMP(M,I)=RI*0.25
0176:       IF(M.EQ.2) TEMP(M,I)=(RITEM+RI)*0.25
0177:    14 CONTINUE
      C
0200:       M=1
0201:    15 J=1
0202:    18 K=1
0203:    19 I=1
0204:    20 U=TEMP(M,I)
      C
      C         S/ALPHA FOR SPECIFIED N III, N II LINES, TEMP.
      C
0205:       EDIFA=EZA-EA(J)
0206:       EDIFB=EZB-EB(K)
0207:       EDIFF=EDIFB-EDIFA
0210:       EDIFF=EDIFF*RNO
```

```
0211:          FE=EXP(EDIFF/U)
0212:          S(J,K,I)=RAT(J,K)*FGW(J,K)*FE
               C
0213:          I=I+1
0214:          IF(I-ITEMP) 20,20,21
0215:       21 K=K+1
0216:          IF(K-NTWO) 19,19,22
0217:       22 J=J+1
0220:          IF(J-NTHR) 18,18,23
               C
0221:       23 CONTINUE
0222:          IF(IPRNT.EQ.0) GO TO 71
0223:          IF(IT.LE.IPST) GO TO 71
0224:          IF(M.EQ.2) GO TO 71
0225:          WRITE(5,106)(TEMP(M,I),I=1,ITEMP)
0226:          WRITE(5,123)
0227:          DO 55 J=1,NTHR
1   0230:          WRITE(5,107)((S(J,K,I),I=1,ITEMP),K=1,NTWO)
11  0231:       55 WRITE(5,101)
0232:          WRITE(5,123)
               C
               C          AVERAGE S/ALPHA & STD. DEV. FOR EACH N III LINE
               C
0233:          WRITE(5,144)
0234:          DO 88 J=1,NTHR
1   0235:          DO 87 I=1,ITEMP
12  0236:          SASUM=0
2   0237:          SADIF=0
22  0240:          RNTWO=NTWO
2   0241:          DO 85 K=1,NTWO
03  0242:       85 SASUM=SASUM+S(J,K,I)
2   0243:          AVSA(I)=SASUM/RNTWO
22  0244:          DO 86 K=1,NTWO
03  0245:       86 SADIF=SADIF+(S(J,K,I)-AVSA(I))**2
12  0246:       87 DEVSA(I)=SQRT(SADIF/(RNTWO-1.0))
1   0247:          WRITE(5,145)
11  0250:          WRITE(5,107)(AVSA(I),I=1,ITEMP)
11  0251:          WRITE(5,107)(DEVSA(I),I=1,ITEMP)
11  0252:       88 CONTINUE
0253:          WRITE(5,123)
0254:       71 CONTINUE
               C
               C          SPECIFY COMBINATION OF N III LINES ( L=LCHK MEANS ALL LINES
               C          CALC. MEAN S/ALPHA FOR EACH COMBINATION ,
               C          STD. DEVN. AND PERCENTAGE STD. DEVN.
               C
0255:          L=1
0256:       24 CONTINUE
0257:          DO 26 I=1,ITEMP
1   0260:          DIFS(I)=0
21  0261:       26 SUM(I)=0
0262:          IF(L.NE.LCHK) NFAC=2
0263:          IF(L.EQ.LCHK) NFAC=NTHR
0264:          N1=NA(L)
0265:          N2=NB(L)
0266:          NINC=NI(L)
0267:          DO 27 I=1,ITEMP
```

```
0270:       DO 37 J=N1,N2,NINC
0271:       DO 37 K=1,NTWO
0272:    37 SUM(I)=SUM(I)+S(J,K,I)
0273:       PROD=NTWO*NFAC
0274:    27 AV(I,M,L)=SUM(I)/PROD
       C
0275:       DO 28 I=1,ITEMP
0276:       DO 38 J=N1,N2,NINC
0277:       DO 38 K=1,NTWO
0300:    38 DIFS(I)=DIFS(I)+(S(J,K,I)-AV(I,M,L))**2
0301:    28 SDEV(I,M,L)=SQRT(DIFS(I)/PROD)
0302:       DO 29 I=1,ITEMP
0303:    29 RELE(I,M,L)=100.0*(SDEV(I,M,L)/AV(I,M,L))
       C
0304:       IF(IPRNT.EQ.0) GO TO 72
0305:       IF(IT.LE.IPST) GO TO 72
0306:       IF(M.EQ.2) GO TO 72
0307:       IF(L.EQ.1.OR.L.EQ.7.OR.L.EQ.13) WRITE(5,133)(TEMP(M,I),I=1,ITEMP
0310:       IWA1=WA(N1)
0311:       IWA2=WA(N2)
0312:       IF(L.NE.LCHK) WRITE(5,108) L,IWA1,IWA2
0313:       IF(L.EQ.LCHK) WRITE(5,109)
0314:       WRITE(5,107) (AV(I,M,L),I=1,ITEMP)
0315:       WRITE(5,111)
0316:       WRITE(5,107) (SDEV(I,M,L),I=1,ITEMP)
0317:       WRITE(5,112)
0320:       WRITE(5,110) (RELE(I,M,L),I=1,ITEMP)
0321:       WRITE(5,124)
0322:    72 CONTINUE
0323:       L=L+1
0324:       IF(L-LCHK) 24,24,30
       C
       C        SECOND BLOCK OF TEMPS.
       C
0325:    30 M=M+1
0326:       IF(M-2) 15,15,31
       C
       C        FIND MIN. PERCENTAGE STD. DEVN. AMONGST TEMP. VALUES
       C        ( BOTH BLOCKS ) FOR EACH COMBINATION NO. L
       C
       C        IOPT=1 : TAKE MIN. STD. DEV.
       C
0327:    31 CONTINUE
0330:       IFIN=ITEMP-1
0331:       DO 33 L=1,LCHK
0332:       M=1
0333:       IF(IOPT.EQ.1) GO TO 49
0334:       DO 39 I=ISTRT,IFIN
0335:       IF(RELE(I+1,M,L).GT.RELE(I,M,L)) GO TO 36
0336:    39 CONTINUE
0337:       IF(RELE(1,2,L).GT.RELE(ITEMP,1,L)) GO TO 36
0340:       M=2
0341:       DO 32 I=1,IFIN
0342:       IF(RELE(I+1,M,L).GT.RELE(I,M,L)) GO TO 36
0343:    32 CONTINUE
       C
0344:    49 CONTINUE
```

```
0345:        DO 41 I=ISTRT,IFIN
0346:        IF(SDEV(I+1,M,L).GT.SDEV(I,M,L)) GO TO 36
0347:     41 CONTINUE
0350:        IF(SDEV(1,M+1,L).GT.SDEV(ITEMP,M,L)) GO TO 36
0351:        M=2
0352:        DO 42 I=1,IFIN
0353:        IF(SDEV(I+1,M,L).GT.SDEV(I,M,L)) GO TO 36
0354:     42 CONTINUE
      C
0355:     36 IMIN=I
0356:        MMIN=M
0357:        TMIN(L)=TEMP(MMIN,IMIN)
0360:        SMIN(L)=AV(IMIN,MMIN,L)
0361:        TSOL(L,IT)=TMIN(L)
0362:        SSOL(L,IT)=SMIN(L)
0363:     33 CONTINUE
0364:        IF(IGAS.EQ.2) GO TO 78
      C
      C        OUTPUT S/ALPHA AND TEMP. AT MIN. FOR EACH L
      C        ( INCLUDING COMBINATION OF ALL LINES )
      C
0365:        LFIN=LCHK-1
0366:        WRITE(5,113) TIME(IT)
0367:        WRITE(5,122) TMIN(LCHK),SMIN(LCHK)
0370:        WRITE(5,114) (L,TMIN(L),SMIN(L),L=1,LFIN)
      C
      C        FIND AVERAGE AND STD. DEV. OF S/ALPHA AND TEMP. OVER L'S
      C        ( EXCLUDING COMBINATION OF ALL LINES )
      C
0371:        TSUM=0
0372:        SSUM=0
0373:        TDIF=0
0374:        SDIF=0
0375:        RLFIN=LFIN
0376:        DO 34 L=1,LFIN
0377:        TSUM=TSUM+TMIN(L)
0400:     34 SSUM=SSUM+SMIN(L)
0401:        TAV(IT)=TSUM/RLFIN
0402:        SAV(IT)=SSUM/RLFIN
0403:        DO 35 L=1,LFIN
0404:        TDIF=TDIF+(TMIN(L)-TAV(IT))**2
0405:     35 SDIF=SDIF+(SMIN(L)-SAV(IT))**2
0406:        DENOM=RLFIN*(RLFIN-1.0)
0407:        DEVT(IT)=SQRT(TDIF/DENOM)
0410:        DEVS(IT)=SQRT(SDIF/DENOM)
0411:        WRITE(5,115) TAV(IT),SAV(IT)
0412:        WRITE(5,116) DEVT(IT),DEVS(IT)
0413:        WRITE(5,123)
      C
0414:        IF(IGAS.EQ.7) GO TO 79
0415:     78 TAV(IT)=TMIN(L)
0416:        SAV(IT)=SMIN(L)
0417:        DEVT(IT)=0
0420:        DEVS(IT)=SDEV(I,M,L)
0421:     79 CONTINUE
      C
      C        MOVE TO NEXT TIME
```

```
      C
0422:       IT=IT+1
0423:       IF(IT-ITEND) 13,13,40
      C
      C           OUTPUT FINAL RESULTS ( TIME , KT & S/ALPHA WITH STD. DEVS. )
      C
0424:    40 WRITE(5,131)
0425:       WRITE(5,132)(TIME(IT),TAV(IT),DEVT(IT),SAV(IT),DEVS(IT),IT=1,ITEND
          1)
0426:       WRITE(5,120)
0427:       WRITE(5,123)
0430:       WRITE(5,140)(TIME(IT),IT=1,ITEND)
0431:       WRITE(5,141)(L,(TSOL(L,IT),IT=1,ITEND),L=1,LFIN)
0432:       WRITE(5,142)(TIME(IT),IT=1,ITEND)
0433:       WRITE(5,143)(L,(SSOL(L,IT),IT=1,ITEND),L=1,LFIN)
0434:       WRITE(5,136)(TIME(IT),IT=1,ITEND)
0435:       DO 77 J=1,NTHR
0436:       WRITE(5,137)((RATIO(J,K,IT),IT=1,ITEND),K=1,NTWO)
0437:       WRITE(5,138)
0440:    77 CONTINUE
0441:       WRITE(5,139)
      C
      C           FORMAT STATEMENTS
      C
0442:    101 FORMAT(' ')
0443:    102 FORMAT(F7.2,F8.3,F6.1,F11.1)
0444:    104 FORMAT(12F7.2)
0445:    105 FORMAT('1',' ',128('-'),//,T56,'TIME = ',F5.2,' USEC',/,T56,17('-'
          1))
0446:    106 FORMAT(' KT',F6.2,15F8.2)
0447:    107 FORMAT(' ',16E8.3)
0450:    108 FORMAT(T5,'COMBIN.NO.',I4,T50,'MEAN S/ALPHA (',I5,',',I5,' )',/,T5
          1,14('-'),T50,28('-'))
0451:    109 FORMAT(T50,'MEAN S/ALPHA (ALL LINES)',/,T50,24('-'))
0452:    110 FORMAT(' ',16F8.3)
0453:    111 FORMAT(T55,'STD. DEVIATION')
0454:    112 FORMAT(T52,'PERCENTAGE STD. DEV.')
0455:    113 FORMAT('1',T50,'SOLUTIONS',T70,'TIME =',F6.2,' USEC',/,T50,37('-')
          1,/,T25,'COMBINATION NO.',T57,'TEMPERATURE',T88,'S/ALPHA',/,T25,15(
          2'-'),T57,11('-'),T88,7('-'))
0456:    114 FORMAT(/,30X,I2,28X,F4.2,20X,E8.3)
0457:    115 FORMAT(/,25X,'FINAL AVERAGE',22X,F4.2,20X,E8.3)
0460:    116 FORMAT(/,25X,'STD. DEV. OF MEAN',18X,F4.2,20X,E8.3)
0461:    117 FORMAT('1',' ',128('-'),///,T60,'LINES USED',/,T60,10('-'),//,T20,
          1'NO.',T45,'WAVELENGTH',T70,'F',T90,'G',T110,'E',/,T20,3('-'),T45,1
          20('-'),T70,'-',T90,'-',T110,'-',//,T10,'N III',/)
0462:    118 FORMAT('0',T20,I2,T45,F9.2,T67,F5.3,T88,F4.1,T107,F8.1)
0463:    119 FORMAT(///,T10,'N II',/)
0464:    120 FORMAT(////)
0465:    122 FORMAT(/,27X,'ALL LINES',24X,F4.2,20X,E8.3,/)
0466:    123 FORMAT('0',129('-'),/)
0467:    124 FORMAT(' ',129('-'))
0470:    125 FORMAT(12F7.2)
0471:    126 FORMAT(12F7.3)
0472:    131 FORMAT('1',' ',128('-'),//,T31,'TIME',T56,'TEMP.',T70,'STD.DEV.',
          1T88,'S/ALPHA',T104,'STD.DEV.',/,T31,4('-'),T56,21('-'),T88,23('-')
          2,//)
```

```
0473:   132 FORMAT('0',T30,F5.2,T56,F5.2,T70,F5.2,T86,E8.3,T102,E8.3)
0474:   133 FORMAT('1',T2,129('-'),/,' KT',F6.2,15F8.2,/,T2,129('-'))
0475:   136 FORMAT('1',128('-'),///,T55,'INTENSITY RATIOS',/,T55,16('-'),//,
          118F7.2,' US',/,129('-'),/)
0476:   137 FORMAT('0',18E7.2)
0477:   138 FORMAT(//)
0500:   139 FORMAT('0',//,128('-'))
0501:   140 FORMAT('1',T40,'TEMP. SOLUTIONS FOR EACH COMBIN. AS FUNCTION OF TI
          1ME',/,T40,52('-'),//,T2,'US',18F7.2,/,129('-'),/)
0502:   141 FORMAT(I3,18F7.2,/)
0503:   142 FORMAT('1',T40,'S/ALPHA SOLUTIONS FOR EACH COMBIN. AS FUNCTION OF
          1TIME',/,T40,54('-'),//,T2,'US',18F7.2,/,129('-'),/)
0504:   143 FORMAT(I3,18E7.2,/)
0505:   144 FORMAT(' ',T44,'AV. S/ALPHA & STD. DEV. FOR EACH N III LINE',/,T44
          1,43('-'))
0506:   145 FORMAT(' ')
        C
0507:       STOP
0510:       END
```

```
:-18:5(-
      C
      C                                  ********************
      C                                  *   PROGRAM RLTE     *
      C                                  ********************
0101:       DIMENSION TEMP(2,16),WA(8),FA(8),GA(8),EA(8),WB(12),FB(12),GB(12),
           1EB(12),A(8),B(12),VA(8),VB(12),PMA(8),PMB(12),FGW(8,12),
           2REXPT(2,16,8,12),RCALC(2,16,8,12),RDIF(2,16,8,12),TSOL(8,12),TIME
           3(20),TAV(20),TDEV(20)
0102:       DIMENSION V(5),IBEG(2),EDENS(20)
0103:       DIMENSION SAHA(18)
      C
0104:       REAL MFAC,NE,NESUB
      C
      C        TIME INTERVAL , NO. OF INTERVALS
0105:       DATA TIMINC,ITEND/0.25,18/
      C        FIRST TRIAL KT NO. , KT INTERVAL
0106:       DATA ISTART/4/TINC/0.20/
      C        CONVERSION CM-1 TO EV , ME / 2 PI HBAR SQUARED
0107:       DATA RNO/ .124E-03/FAC/ .20864E+15/
      C        VARIABLE FORMAT PARAMETERS
0110:       DATA V(1),V(3),V(5)/'(1H+,','X,','E8.3)'/
0111:       DATA IBEG/1,1/V(2),V(4)/'1','16'/IST/3/
      C        ION CHARGE NO. , ELECTRONIC CHARGE / EPSILON NOUGHT ,
      C        N III IONIZATION ENERGY , N III / N IV GROUND STATE
      C                                  STATISTICAL WEIGHTS
0112:       DATA Z/3.0/EOEP/ .2433E-12/PI/3.142/EUP/47.426/GZ/2.0/
      C        N II IONIZATION ENERGY
0113:       DATA EZ/238751.1/
      C        NOS. OF N II LINES , N III LINES , KT INTERVALS ( IN EACH
      C                                  OF TWO BLOCKS )
0114:       DATA NTWO,NTHR,ITEMP/9,7,16/
      C        ELECTRON DENSITY DATA SET NO.
0115:       DATA NESET/21/NESUB/' '/
      C        TIME INTERVAL NO. TO START PRINTING DETAILED CALCS.
0116:       DATA IPST/15/
      C
      C        INPUT ELECTRON DENSITY DATA
      C        INPUT FIXED DATA ARRAY : WAVELENGTH , F , G , ENERGY
      C        ( J = N III LINE INDEX , K = N II LINE INDEX )
      C
0117:       READ(8,101)(EDENS(IT),IT=1,ITEND)
0120:       DO 11 J=1,NTHR
0121:    11 READ(8,102) WA(J),FA(J),GA(J),EA(J)
0122:       DO 12 K=1,NTWO
0123:    12 READ(8,102) WB(K),FB(K),GB(K),EB(K)
      C
0124:       DO 61 J=1,NTHR
0125:       DO 61 K=1,NTWO
0126:       FGW(J,K)=FA(J)*GA(J)*((WB(K)/WA(J))**3)/(FB(K)*GB(K))
0127:    61 CONTINUE
      C
      C        INPUT VOLTAGE SCALE FACTORS , PM RESPONSE FACTORS
      C
0130:       READ(8,125)(VA(J),J=1,NTHR)
0131:       READ(8,125)(VB(K),K=1,NTWO)
0132:       READ(8,126)(PMA(J),J=1,NTHR)
```

```
0133:       READ(8,126)(PMB(K),K=1,NTWO)
      C
0134:       WRITE(5,117)
0135:       WRITE(5,118)(J,WA(J),FA(J),GA(J),EA(J),J=1,NTHR)
0136:       WRITE(5,119)
0137:       WRITE(5,118)(K,WB(K),FB(K),GB(K),EB(K),K=1,NTWO)
0140:       WRITE(5,123)
0141:       WRITE(5,127) NESET,NESUB,(EDENS(IT),IT=1,ITEND)
      C
      C          SET TIME ; INPUT INTENSITIES
      C
0142:       IT=1
0143:    13 T=IT
 144:       TIME(IT)=T*TIMINC
 145:       READ(8,104)(A(J),J=1,NTHR)
 146:       READ(8,104)(B(K),K=1,NTWO)
      C
      C          MULTIPLY BY FACTORS
      C
 147:       DO 51 J=1,NTHR
 150:       A(J)=A(J)*VA(J)
 151:       A(J)=A(J)*PMA(J)
 152:    51 CONTINUE
 153:       DO 52 K=1,NTWO
 154:       B(K)=B(K)*VB(K)
 155:       B(K)=B(K)*PMB(K)
 156:    52 CONTINUE
      C
      C          WRITE TIME , TEMPERATURE VALUES ; CALCULATE EXPERIMENTAL
      C                          LINE INTENSITY RATIOS
      C
 157:       IF(IT.LE.IPST) GO TO 54
 160:       WRITE(5,105) TIME(IT)
 161:    54 CONTINUE
      C
 162:       DO 14 M=1,2
 163:       DO 14 I=1,ITEMP
 164:       RI=I+ISTART-1
 165:       RITEM=ITEMP
 166:       IF(M.EQ.1) TEMP(M,I)=RI*TINC
 167:       IF(M.EQ.2) TEMP(M,I)=(RITEM+RI)*TINC
 170:    14 CONTINUE
 171:       DO 62 J=1,NTHR
 172:       DO 62 K=1,NTWO
 173:       DO 62 M=1,2
 174:       ISTRT=IBEG(M)
 175:       DO 62 I=ISTRT,ITEMP
 176:    62 REXPT(M,I,J,K)=A(J)/B(K)
      C
 177:       M=1
 200:    15 CONTINUE
 201:       IF(IT.LE.IPST) GO TO 53
 202:       IF(M.EQ.2) GO TO 53
 203:       WRITE(5,106)(TEMP(M,I),I=1,ITEMP)
 204:    53 CONTINUE
      C
      C          CALCULATE THEORETICAL LINE INTENSITY RATIO FROM LTE RELATION ,
```

```
C          FIND DIFFERENCE AND OUTPUT THEORETICAL - EXPERIMENTAL RATIOS
C          AND DIFFERENCE FOR EACH COMBINATION OF LINES
C
0205:          J=1
0206:       18 K=1
0207:       19 I=IBEG(M)
0210:       20 U=TEMP(M,I)
0211:          NE=EDENS(IT)
0212:          MFAC=(FAC*U)**1.5
0213:          FE=EXP((EZ+EA(J)-EB(K))*RNO/U)
0214:          RCALC(M,I,J,K)=2.0*(MFAC/NE)*FGW(J,K)/FE
0215:          RDIF(M,I,J,K)=ABS(RCALC(M,I,J,K)-REXPT(M,I,J,K))
0216:          I=I+1
0217:          IF(I-ITEMP) 20,20,21
0220:       21 K=K+1
0221:          IF(K-NTWO)19,19,22
0222:       22 J=J+1
0223:          IF(J-NTHR)18,18,23
0224:       23 CONTINUE
0225:          IF(IT.LE.IPST) GO TO 55
0226:          IF(M.EQ.2) GO TO 55
0227:          DO 63 J=1,NTHR
0230:          DO 63 K=1,NTWO
0231:          IF(J.EQ.2.AND.K.EQ.5) WRITE(5,129)
0232:          IF(J.EQ.4.AND.K.EQ.1) WRITE(5,129)
0233:          IF(J.EQ.5.AND.K.EQ.6) WRITE(5,129)
0234:          IF(J.EQ.7.AND.K.EQ.2) WRITE(5,129)
0235:          IF(M.EQ.1) GO TO 99
0236:          WRITE(5,131)(RCALC(M,I,J,K),I=1,ITEMP)
0237:          WRITE(5,132)(REXPT(M,I,J,K),I=1,ITEMP)
0240:          WRITE(5,133)(RDIF(M,I,J,K),I=1,ITEMP)
0241:          GO TO 98
0242:       99 ISTR=IBEG(1)
0243:          WRITE(5,191)
0244:          WRITE(5,V)(RCALC(M,I,J,K),I=ISTR,ITEMP)
0245:          WRITE(5,192)
0246:          WRITE(5,V)(REXPT(M,I,J,K),I=ISTR,ITEMP)
0247:          WRITE(5,193)
0250:          WRITE(5,V)(RDIF(M,I,J,K),I=ISTR,ITEMP)
0251:       98 CONTINUE
0252:       63 CONTINUE
C
C          SECOND BLOCK OF TEMPERATURES
C
0253:          WRITE(5,123)
0254:          IF(M.EQ.1) WRITE(5,129)
0255:       55 M=M+1
0256:          IF(M-2)15,15,31
C
C          FOR EACH COMBINATION FIND TEMPERATURE AT WHICH DIFFERENCE IS A
C               MINIMUM AND OUTPUT TEMPERATURE SOLUTION
C
0257:       31 WRITE(5,150) TIME(IT)
0260:          IFIN=ITEMP-1
0261:          DO 66 J=1,NTHR
0262:          DO 66 K=1,NTWO
0263:          M=1
```

```
0264:        DO 64 I=IST,IFIN
0265:        IF(RDIF(M,I+1,J,K).GT.RDIF(M,I,J,K)) GO TO 36
0266:     64 CONTINUE
0267:        IF(RDIF(2,1,J,K).GT.RDIF(1,ITEMP,J,K)) GO TO 36
0270:        M=2
0271:        DO 65 I=1,ITEMP
0272:        IF(RDIF(M,I+1,J,K).GT.RDIF(M,I,J,K)) GO TO 36
0273:     65 CONTINUE
0274:     36 IMIN=I
0275:        MMIN=M
0276:        TSOL(J,K)=TEMP(MMIN,IMIN)
0277:        IWA=WA(J)
0300:        IWB=WB(K)
0301:        WRITE(5,151) IWA,IWB,TSOL(J,K)
0302:     66 CONTINUE
C
C          CALCULATE AND OUTPUT AVERAGE TEMPERATURE SOLUTION AND ITS
C               STANDARD DEVIATION OVER ALL LINES
C
0303:        TSUM=0
0304:        TDIF=0
0305:        DO 71 J=1,NTHR
0306:        DO 71 K=1,NTWO
0307:     71 TSUM=TSUM+TSOL(J,K)
0310:        PROD=NTHR*NTWO
0311:        TAV(IT)=TSUM/PROD
0312:        DO 72 J=1,NTHR
0313:        DO 72 K=1,NTWO
0314:     72 TDIF=TDIF+(TSOL(J,K)-TAV(IT))**2
0315:        TDEV(IT)=SQRT(TDIF/(PROD*(PROD-1)))
0316:        WRITE(5,123)
0317:        WRITE(5,152) TAV(IT),TDEV(IT)
0320:        WRITE(5,123)
C
C          CALCULATE SAHA RATIO
C
0321:        DELE=Z*EUEP*(SQRT(NE/TAV(IT)))/(4.0*PI)
0322:        SAHA(IT)=2.0*(FAC*TAV(IT))**1.5/(NE*GZ*EXP((EUP-DELE)/TAV(IT)))
C
C          MOVE TO NEXT TIME
C
0323:        IT=IT+1
0324:        IF(IT-ITEND) 13,13,40
C
C          OUTPUT AVERAGE TEMPERATURE AND STANDARD DEVIATION FOR ALL TIMES
C
0325:     40 WRITE(5,153)
0326:        WRITE(5,154)
0327:        DO 41 IT=1,ITEND
0330:     41 WRITE(5,155) TIME(IT),TAV(IT),TDEV(IT),EDENS(IT),SAHA(IT)
0331:        WRITE(5,123)
C
C          FORMAT STATEMENTS
C
0332:    101 FORMAT(6E11.2)
0333:    102 FORMAT(F7.2,F8.3,F6.1,F11.1)
0334:    104 FORMAT(12F7.2)
```

```
0335:    105 FORMAT('1',T58,'TIME =',F6.2,' USEC')
0336:    106 FORMAT(' ',129('-'),/,T2,'KT',F6.2,15F8.2,/,T2,129('-'))
0337:    117 FORMAT('1',T60,'LINES USED',/,T60,10('-'),//,T20,
           1'NO.',T45,'WAVELENGTH',T70,'F',T90,'G',T110,'E',/,T20,3('-'),T45,1
           20('-'),T70,'-',T90,'-',T110,'-',//,T10,'N III',/)
0340:    118 FORMAT('0',T20,I2,T45,F9.2,T67,F5.3,T88,F4.1,T107,F8.1)
0341:    119 FORMAT(///,T10,'N II',/)
0342:    123 FORMAT('0',128('-'))
0343:    125 FORMAT(12F7.2)
0344:    126 FORMAT(12F7.3)
0345:    127 FORMAT('0',T40,'NE VALUES ( FROM DATA',I3,' / 73 (',A1,') )',//,T40
           1,35('-'),/,T2,18(1PE7.1),//,129('-'))
0346:    129 FORMAT('1')
0347:    131 FORMAT('0C',16E8.3)
0350:    132 FORMAT(' E',16E8.3)
0351:    133 FORMAT(' D',16E8.3)
0352:    150 FORMAT('1',T2,'TIME =',F5.2,T38,'N III / N II',T83,'TEMPERATURE',/
           1,T2,11('-'),T38,12('-'),T83,11('-'),/)
0353:    151 FORMAT(T39,I4,' / ',I4,T86,F5.2)
0354:    152 FORMAT(/ ,T28,'AVERAGE TEMPERATURE (ALL LINES)',T86,F5.2,//,T30,'S
           1TANDARD DEVIATION OF MEAN',T86,F5.2)
0355:    153 FORMAT('1',T2,128('-'),////)
0356:    154 FORMAT(T20,'TIME',T45,'TEMPERATURE',T70,'ELECTRON DENSITY',T95,
           1'SAHA RATIO',/,T20,4('-'),T45,11('-'),T70,16('-'),T95,10('-'),/)
0357:    155 FORMAT('0',T20,F4.2,T43,F8.2,F6.2,T70,1PE11.1,T95,E9.2)
0360:    191 FORMAT('0C')
0361:    192 FORMAT(' E')
0362:    193 FORMAT(' D')
         C
0363:        STOP
0364:        END
```